PETROLOGY, GEOCHEMISTRY AND Sr-Nd ISOTOPES OF THE PALEOPROTEROZOIC MAFIC DYKES FROM THE GOIÁS-CRIXÁS ARCHEAN BLOCK, GOIÁS STATE, BRAZIL

PAULO CESAR CORRÊA DA COSTA & *VICENTE A. V. GIRARDI

Resumo Diques máficos paleoproterozóicos que intrudem os terrenos do bloco arqueano Goiás-Crixás compreedem dois grupos de toleitos: os de alto Ti (HTi – TiO_2>1,5%) e os de baixo Ti (TiO_2<1,5%). Os valores de mg# de HTi e LTi variam respectivamente de 0,49 a 0,31 e de 0,33 a 0,18. HTi é enriquecido em LILE (Rb, Ba, Sr) e LREE (La, Ce) em relação a LTi. Os padrões e as razões de elementos incompatíveis (IE) de HTi são aproximadamente intermediárias entre E-MORB e OIB, enquanto LTi aproxima-se de E-MORB, mas tem também características de N-MORB. Entretanto as anomalias de Nb são sempre negativas. O estudo da origem de HTi e LTi mostrou que a única explicação possível é a heterogeneidade mantélica. Tendo-se em conta ambos os grupos, a razão inicial $^{87}Sr/^{86}Sr$ (Sr_i) varia de 0,700 a 0,705 correspondendo a εSr –21,89 a + 46,52, enquanto que a variação da razão inicial $^{143}Nd/^{144}Nd$ (Nd_i) é de 0,5092 a 0,5120, relativa a εåNd – 4,84 a + 0,53, considerando-se a idade de 2.49 Ga. Esses valores e os dados geoquímicos sugerem fonte constituída pela mistura de manto empobrecido e componente EMI. Sugere-se que a assinatura isotópica EMI deva-se a crosta oceânica, contendo eclogitos e sedimentos, subductada durante o Arqueano ou o Paleoproterozóico. Fluidos e/ou fusões metassomáticos provenientes dos eclogitos provocaram diferentes graus de enriquecimento em elementos incompatíveis na fonte mantélica, originando HTi e LTi. A anomalia negativa de Nb em relação a LILE e LREE deve-se à sua retenção em rutilo dos eclogitos. As anomalias positivas de Ba podem ser atribuídas a sedimentos pelágicos da crosta oceânica. A similaridade entre os dados geoquímicos e isotópicos dos diques de Goiás e outros dos Cratons Amazônico e São Francisco sugerem ambiente continental.

Palavras-chave: diques máficos, Goiás, manto, metassomatismo

Abstract Paleoproterozoic mafic dyke swarm that intruded the Goiás-Crixás Archean Block comprises two groups of dykes: the high Ti (HTi - TiO_2 >1.5%) and the low Ti (TiO_2 < 1.5%) tholeiites. HTi and LTi have mg# values ranging from 0.49 to 0.31 and from 0.33 to 0.18 respectively. HTi is enriched in LILE (Rb, Ba, K) and LREE (La, Ce) with respect to LTi. HTi incompatible trace elements (IE) patterns and ratios are broadly intermediate between E-MORB and OIB, whereas LTi is closer to E-MORB, but exhibits some N-MORB features. However Nb anomalies are always negative. The studies on the origin of HTi and BTI reveled that mantle heterogeneity is the only possible explanation. The initial $^{87}Sr/^{86}Sr$ (Sr_i) ranges from 0.700 to 0.705 (åSr –21.89 to + 46.52) and the initial $^{143}Nd/^{144}Nd$ (Nd_i) varies from 0.5092 to 0.5120 (åNd – 4.84 to + 0.53) at 2.49 Ga. Isotopic and geochemical data suggest a mixed parental source constituted by DMM and EMI components. It is suggested that the EMI signature originates from an oceanic slab containing eclogites and sediments, subducted during Paleoproterozoic or Archean times. Metasomatic fluids and/or melts from the eclogites account for greater and lesser IE mantle enrichment, giving rise to HTi and LTi respectively. The Nb depletion relative to LILE and LREE is due to retention by rutile of eclogites, and characterizes continental and IAB tholeiites. The positive spikes of Ba in HTi can be attributed to pelagic sediments of the slab. The similarity between geochemical and isotopic data of the Goiás dykes and others from the São Francisco and Amazonic cratons suggest a similar continental environment.

Keywords: mafic dykes, Goiás, mantle, metasomatism.

INTRODUCTION Many articles have stressed the importance of geochemical and isotopic studies of mafic dykes as guides to petrogenetic processes and geochemical characteristics of the parental source mantle. These data can also indicate the geotectonic setting of the basic bodies. In the South-American Platform the researches have been carried out on Mesozoic and mainly on Proterozoic dykes swarms, in the Amazonic (Rivalenti *et al.* 1998, Menezes Leal et al. 2000), São Francisco (Bellieni *et al.* 1991, 1995, 1998, Menezes Leal *et al.* 1995, Pinese 1997, Mazzucchelli *et al.* 2001) and in the Rio da Plata Cratons (Bossi *et al.* 1993, Rivalenti *et al.* 1995, Mazzucchelli *et al.* 1995, Girardi *et al.* 1996, Iacumin *et al.* 2001). Iacumin *et al.* (2003) compare several Precambrian and Mesozoic dykes in order to discuss mantle processes and heterogeneity.

The mafic dykes intrude country rocks of the Goiás-Crixás Archean Block (Pimentel *et al.* 2003, 2004). The Archean Block is in contact with Proterozoic units (fig. 1), which comprise folded metamorphic rocks of the Araxá and Serra da Mesa Groups to the east, and Neoproterozoic rocks of the Goiás Magmatic Arc to the north, east and south. The Archean Block is made up of granite-gneiss complexes and greenstone belts sequences. According to several authors the age range of the granite-gneiss complexes is 2.6 - 3.0 Ga (Hasui & Almeida 1970, Tassinari & Montalvão 1980, Vargas 1992, Tomazzoli 1992 and Pimentel *et al.* 2003). Based on SHRIMP U-Pb analyses in zircons and Sm-Nd data Queiroz (2000) and Pimentel *et al.* (2003, 2004) proposed an evolutionary model for the region. According to these authors the sialic crust (3.15-3.30 Ga) is older than the basal sequence of the greenstone belts (ca. 3.0 Ga). However, the age of their top metasedimentary sequences is not known, and probably it is not Archean. The older granitic body yields age of 2.94 Ga. The age of the other granites varies from 2.85 to 2.71 Ga. The oldest bodies underwent a main metamorphic event at 2.79-2.71 Ga. Further metamorphic imprints were registered at 2.0 and 0.59 Ga (Queiroz 2000). According to the data by Queiroz (2000) and Pimentel *et al.* (2003,2004) the dyke swarm crosscuted granite-gneiss complexes yielding ages

– Instituto de Geociências da Universidade de S. Paulo - Rua do Lago, 562 - Cidade Universitária – 05508-080 S. Paulo.
*Corresponding author – girardi@usp.br - tel. (011) 30914095

of 2.71-2.94 Ga.

This swarm has been studied by several authors (e.g. Kuyumjian 1991, 1998, Girardi *et al.* 1992, Tomazzoli 1997, Corrêa da Costa *et al.* 2002, 2003). Based on geochemical and the Sr-Nd isotopic data, this paper discusses the processes responsible for the origin of the mafic magmas, the geochemical and isotopic characteristics of the source mantle, and the geotectonic setting of the dykes. These data will allow the comparison between the mafic dykes of Goiás with those of other cratonic areas of the South-American Platform.

GEOLOGICAL DATA, PETROGRAPHY AND CLASSIFICATION OF THE DYKES The dykes occur within the Crixás-Goiás area (Fig. 1). They trend mainly NE and also NW, and the widths generally vary from 10-15 to 50 m, but sometimes reach 100m. They were classified into three petrographIc groups: diabase, metabasite and amphibolite. Diabases are composed of plagioclase, clinopyroxene and minor amounts of orthopyroxene and amphibole in equilibrium with the other minerals. Textures are ophitic and sub-ophitic. These textures characterize also the metabasites, but in these the pyroxene is largely replaced by secondary amphibole. Quartz-K-feldspar intergrowths occur in both groups. Amphibolites are made up of hornblende, plagioclase, quartz and display granoblastic and nematoblastic textures. Biotite, apatite, zoizite, zircon, titanite and opaques are accessory phases of the three groups.

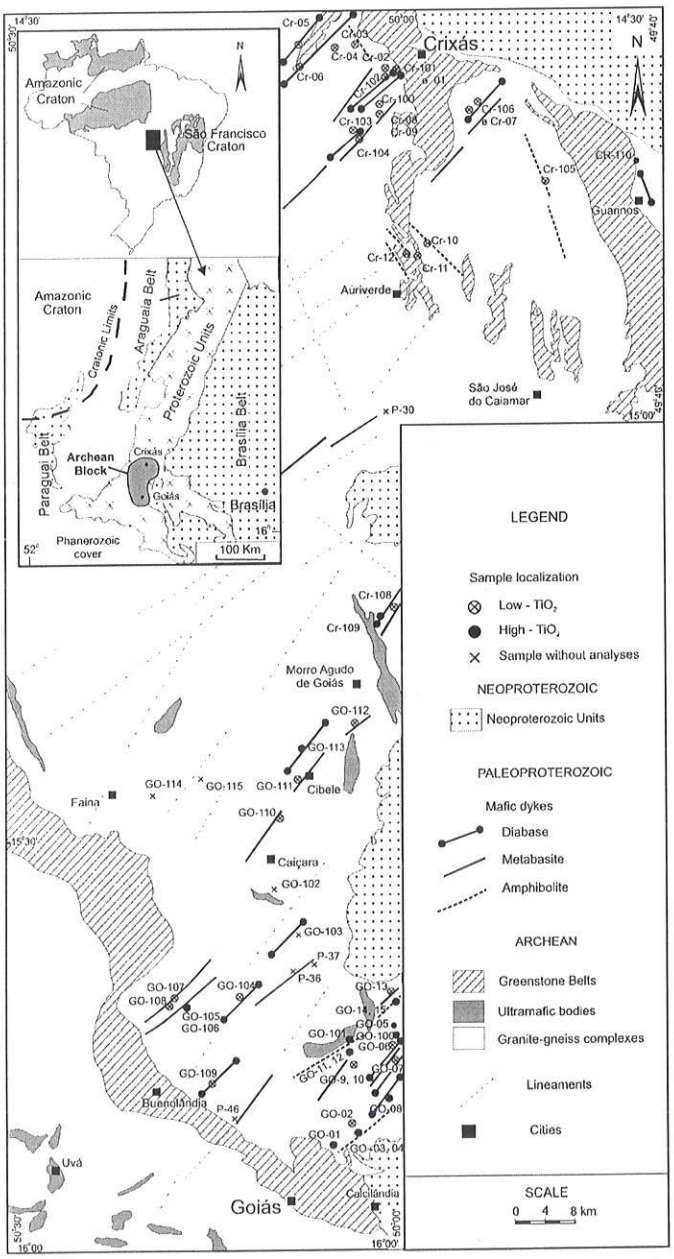

Figure 1- Geological map of the Goiás – Crixás region (modified after Lacerda Filho et al. 2000).

Table 1 shows the whole-rock analyses. The dyke suites have tholeiitic affinity and the majority of the rocks are classified as basalts, but some of the samples, mainly diabases, are basaltic andesites. Corrêa da Costa & Girardi (2004) report detailed descriptions on the mineral chemistry, petrography, classification and crystallization temperatures of diabases and metabasites, which have averages values of 1100-1200° C.

^{39}Ar-^{40}Ar and Rb/Sr data indicate an age of approximately -2,49 Ga for the crystallization of the diabases (Corrêa da Costa *et al.* 2003).

ANALYTICAL PROCEDURES Major and trace elements were determined by X-ray fluorescence in the Dipartimento di Scienze Della Terra, Università di Modena e Reggio Emilia, Itália, by using the analytical procedure of Franzini et al. (1975) and Leoni & Saitta (1976). Analyses are accurate within 2-5% for major elements and better than 10% for trace elements. Rare earth elements (REE) analyses were carried out using neutron activation analyses in the Actlab Laboratories, Ontario, Canada. Fe was determined as Fe_2O_3t, and FeO was calculated assuming the ratio $Fe_2O_3/FeO = 0.15$.

The Rb-Sr and Sm-Nd analysis were performed using the methods described by Kawashita (1972) modified by Sato et al. (1995), involving HF-HNO_3 dissolution plus HCl cation exchange separation. No visible solid residues were observed after dissolution. The Sr isotopic ratios were normalized to $^{86}Sr/^{88}Sr = 0.1194$; replicate analyses of $^{87}Sr/^{86}Sr$ for the NBS987 standard gave a mean value of 0.71028 ± 0.00006 (2s), the blanks for Sr were 5 ng. Nd ratios were normalized to $^{146}Nd/^{144}Nd = 0.72190$. The averages of $^{143}Nd/^{144}Nd$ for La Jolla and BCR-1 standards were 0.511847 ± 0.00005 (2s) and 0.512662 ± 0.00005 (2s), respectively. Sr and Nd isotopic analysis were carried out on a multicollector VG 354 Micromass and Finnigan-MAT 262 mass spectrometers respectively. The isotopic data were regressed using the Isoplot program by Ludwig (1999).

GEOCHEMISTRY Whole-rock Geochemistry Molecular proportion ratio (MPR) diagrams (Pearce 1968, Beswick 1982) were used in order to check possible post-magmatic effects on the original igneous geochemistry of the dykes. In closed systems, elements fractionated during crystallization, normalized to elements that are not contained in the fractionated phases, define regression lines having slopes equal to the ratio of the fractionated elements in the removed phases. Straight lines that do not pass through the origin of the diagrams characterize igneous trends. Figure 2 displays some examples of these plots, which indicate the

maintenance of the igneous trends. Therefore post-magmatic events did not affect significantly the igneous geochemistry.

The highest mg# value [mg # = atomic $Mg^{2+}/(Mg^{2+} + Fe^{2+})$, assuming $Fe_2O_3/FeO = 0.15$] of the suite is 0.49, which means that the magmas are evolved. Primary mantle derived basaltic magmas, would have mg# values 0.74-0.80 (Jaques & Green 1979, Takahashi & Kushiro 1983). The dykes were divided into two groups: 1- high Ti (HTi - $TiO_2 > 1.5\%$) 2 – low Ti (LTi- $TiO_2 < 1.5\%$). In general, HTi prevails in the southern part of the investigated area, while LTi occurs both in northern and southern portions. LTi has mg# from 0.49 to 0.31, while in HTi mg# values vary between 0.33 and 0.18. In both groups, Fe_2O_3t, P_2O_5, K_2O, Na_2O, Zr, Y, La, Nb, Ba, Zn, Ce increase with decreasing mg#, while Al_2O_3, CaO, Cr and Ni decrease. Sr is often constant (Figs. 3 and 4). These trends are compatible with gabbro fractionation. HTi dykes are richer than LTi in Fe_2O_3t, P_2O_5, K_2O, Na_2O, Zr, Y, Nb, Zn, Nd and Ce.

Figure 5 displays the difference in incompatible element contents of both types of dykes normalized to the primordial mantle values (McDonough & Sun 1995). Diabases and metabasites are more fractionated than amphibolites. The HTi group is enriched in LILE (Rb, Ba, K) and LREE (La, Ce) with respect to LTi. Incompatible element patterns (IE) normalized to the primordial mantle are compared with MORB concentrations and patterns (Sun & McDonough 1989). Several average ratios of the LTi group display patterns and average ratios similar to E-MORB (e. g. La/Y, Zr/Y, Ce/Y, Ti/Y, Ce/Zr). However some IE ratios (e.g. P/Nb, Ti/Zr, Ti/P, P/Y) are intermediate between N-MORB and E-MORB (Fig. 5 and Table 2). Negative spikes of Nb are always present in LTi. HTi dykes display IE concentrations and patterns broadly intermediate between E-MORB and OIB, as shown by Fig. 5 and by several average ratios (e.g. La/Y, Ce/Y, Zr/Y, Ti/Zr, Ti/Y, Ti/P, P/Y in Table 2). Nb in all rocks and Sr, except for one sample, have negative anomalies. Ba exhibits positive spikes. The depletion of HSFE, particularly Nb, relative to the enrichment in LILE is a geochemical characteristic that distinguishes basalts from island arcs (IAB) and continental areas from those produced at MORB and OIB; whereas positive Ba anomalies are attributed to pelagic sediments (Weaver 1991) or to some eclogites (Philippot & Selverstone 1991). The REE patterns show that the HTi suite is enriched with respect to LTi. HTi Ce/Yb (5.63 – 24.63) and Sm/Yb (1.14 - 3.13) ratios are intermediate between OIB (Ce/Yb = 37.0, Sm/Yb = 4.62) and E-MORB (Ce/Yb = 6.94, Sm/Yb = 1.09). LTi ratios (Ce/Yb = 3.12 - 10.80 and Sm/Yb = 0.86 – 1.35) and patterns are broadly similar to E-MORB (Corrêa da Costa 2003).

Isotope Geochemistry The initial $^{87}Sr/^{86}Sr$ (Sr_i), $^{143}Nd/^{144}Nd$ (Nd_i) ratios, å(Sr) and å(Nd) of each sample were calculated at 2.4 Ga (Corrêa da Costa et al. 2003). Sr_i varies from 0.70055 to 0.70413 and from 0.70374 to 0.70541 in LTi and Hti, respectively. The åSr range is -15.9 to +34.9 in LTi and + 29.4 to + 53.2 in HTi (Table 2). The variation of Nd_i (0.509322 – 0.509552) and å Nd (–4.1 to + 0.49) is smaller in LTi. In HTi Nd_i and åNd values are 0.509260 and – 5.2 respectively (Table 3).

ESr versus ENd diagram (Fig. 6) reveals that most of the samples plot near to the " Bulk Earth", varying from fairly depleted to enriched with respect to ESr. In terms ofENd, except for one sample (CR-107), they are slightly depleted. Samples from the basement gneisses, calculated at 2.7 Ga plot close to those of the dykes. The Sr_i and Nd_i values range from 0.70418 to 0.70815 and 0.510942 to 0.510995 respectively.

Isotope Geochemistry The initial $^{87}Sr/^{86}Sr$ (Sr_i), $^{143}Nd/^{144}Nd$ (Nd_i) ratios, å(Sr) and å(Nd) of each sample were calculated at 2.49 Ga . Sr_i varies from 0.70003 to 0.70405 and from 0.70314 to 0.70483 in LTi and HTi, respectively. The åSr range is – 21.89 to +35.39 in LTi and + 22.55 to + 46.52 in HTi (Table 3). The variation of Nd_i is

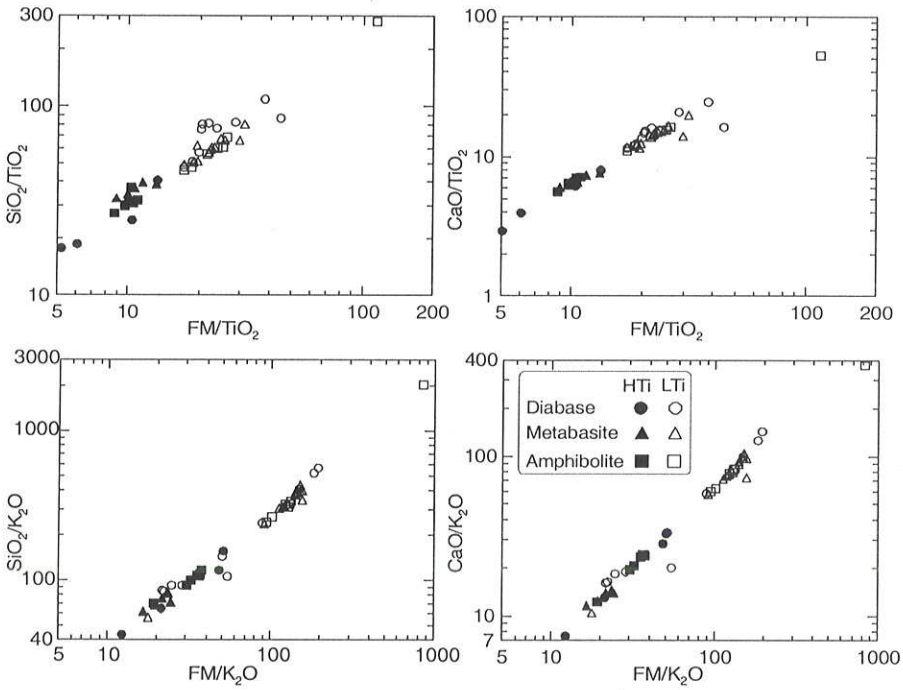

Figure 2- MPR plots of SiO_2/TiO_2 and CaO/TiO_2 vs. FM/TiO_2 and $SiO_2/K2O$ and CaO/K_2O vs. FM/K_2O.

Table 1 - Bulk rock composition of the Goiás samples. < elements below the detection limit. – elements not analyzed.

	Diabase														Metabasite										
Sample	CR01	CR05	CR101	CR102	CR103	CR107	CR109	CR110	GO05	GO06	GO07	GO104	GO109	GO113	CR02	CR07	CR08	CR09	CR100	CR104	CR106	CR108	GO11	GO12	GO13
SiO_2(%)	53.55	52.30	54.00	54.30	49.80	50.00	50.40	45.10	49.70	49.30	49.50	50.10	49.80	48.20	49.90	50.40	50.00	50.00	50.00	50.00	51.10	50.10	51.90	51.10	51.70
TiO_2	0.88	0.91	0.95	0.90	1.39	1.17	3.79	2.40	1.63	1.29	0.76	0.81	0.61	3.43	1.16	1.18	1.32	1.30	1.10	1.35	1.01	1.31	2.01	2.08	1.11
Al_2O_3	14.15	14.46	13.95	14.46	13.54	14.36	12.76	15.49	14.01	13.81	10.96	16.07	16.18	12.64	12.45	12.19	12.51	12.00	12.94	13.88	12.59	12.42	10.46	11.80	13.92
FeO	10.11	10.14	10.35	9.99	11.86	11.19	12.82	13.22	13.18	11.87	10.95	8.78	9.56	15.40	11.54	11.79	11.96	12.55	11.59	11.48	11.72	12.19	16.18	15.74	12.26
FeOT	10.33	10.36	10.57	10.20	12.11	11.43	13.09	13.50	13.46	12.12	11.18	8.97	9.76	15.73	11.79	12.04	12.21	12.81	11.83	11.72	11.97	12.45	16.52	16.07	12.53
Fe_2O_3	1.37	1.37	1.40	1.35	1.60	1.51	1.73	1.78	1.78	1.60	1.48	1.19	1.29	2.08	1.56	1.59	1.61	1.69	1.56	1.55	1.58	1.65	2.18	2.12	1.66
Fe_2O_3T	11.48	11.51	11.75	11.34	13.46	12.70	14.55	15.00	14.96	13.47	12.43	9.97	10.85	17.48	13.10	13.38	13.57	14.24	13.15	13.03	13.30	13.84	18.36	17.86	13.92
MnO	0.17	0.17	0.17	0.17	0.18	0.18	0.18	0.18	0.18	0.18	0.18	0.16	0.17	0.20	0.18	0.18	0.18	0.19	0.18	0.18	0.18	0.19	0.20	0.19	0.19
MgO	6.73	7.87	6.71	6.43	8.45	8.24	6.01	8.61	6.78	8.65	13.58	8.82	8.77	5.74	9.52	9.38	9.00	9.26	9.15	8.29	8.89	8.98	5.27	4.52	7.08
CaO	9.88	9.91	9.74	9.56	11.21	11.17	7.76	10.31	9.21	11.06	8.66	11.91	10.43	9.44	11.66	11.45	11.53	11.29	11.43	11.11	11.14	11.15	8.89	8.85	8.88
Na_2O	2.41	2.31	2.33	2.41	1.91	2.12	2.50	2.48	2.69	1.93	1.25	1.84	2.41	2.32	1.70	1.57	1.72	1.46	1.84	2.07	1.70	1.82	2.52	2.84	2.33
K_2O	0.91	0.89	1.01	1.00	0.19	0.15	1.83	0.61	1.20	0.32	0.73	0.14	0.54	0.48	0.24	0.25	0.21	0.33	0.20	0.18	0.21	0.26	1.20	1.30	1.43
P_2O_5	0.14	0.14	0.17	0.17	0.16	0.15	0.61	0.48	0.26	0.13	0.07	0.08	0.12	0.43	0.11	0.12	0.12	0.14	0.14	0.18	0.14	0.15	0.37	0.39	0.20
LOI	0.20	0.15	0.39	0.13	0.17	0.10	1.98	0.13	0.88	0.21	1.08	0.19	1.14	0.75	0.91	0.75	0.97	0.65	0.62	0.01	0.61	0.66	0.85	0.58	1.04
Total	100.82	100.50	100.84	100.83	100.32	100.30	101.01	100.71	100.70	100.22	98.12	99.93	99.93	100.85	100.03	100.17	100.24	100.23	100.14	100.35	100.34	100.29	101.26	101.02	100.77
Ba(ppm)	269	261	327	273	47	39	573	408	496	51	59	47	320	131	57	103	53	66	58	48	54	64	303	360	484
Rb	29	28	33	22	4	4	28	11	29	15	17	4	8	8	17	16	11	16	15	7	13	8	41	49	44
Sr	198	195	203	197	116	108	713	318	311	122	105	116	335	209	128	125	126	121	121	116	120	118	174	183	398
Cs	-	-	-	0.80	0.07	0.30	0.40	0.40	-	-	-	0.20	0.20	0.10	-	-	-	-	-	0.30	-	0.40	-	-	-
Ga	-	-	-	17.00	20.00	18.00	26.00	22.00	-	-	13	14.00	13.00	24.00	-	-	-	-	-	20.00	-	18.00	-	-	-
Tl	-	-	-	0.13	0.07	<0.05	0.13	0.10	-	-	-	<0.05	0.05	<0.05	-	-	-	-	-	0.10	-	0.08	-	-	-
Nb	4.00	4.00	4.00	4.30	3.50	2.40	25.00	16.00	10.00	<2	2	2.10	3.50	14.70	3.00	4.00	2.00	2.00	<2	3.40	4.00	3.50	16.00	17.00	7.00
Zr	107	112	112	91	79	62	256	166	182	83	45	42	45	196	77	77	89	93	77	77	73	76	320	312	139
Ti	5276	5455	5695	5396	8333	7014	22721	14388	9772	7734	4556	4856	3657	20563	6954	7074	7913	7794	6595	8093	6055	7853	12050	12470	6654
Y	24.00	21.00	32.00	23.30	28.30	23.10	39.10	34.20	34.00	27.00	13	14.50	14.40	47.60	26.00	25.00	27.00	32.00	25.00	27.80	25.00	26.00	62.00	61.00	28.00
Ta	-	-	-	0.37	0.25	0.17	1.85	0.97	-	-	-	0.12	0.17	0.97	-	-	-	-	-	0.26	-	0.24	-	-	-
Th	-	-	-	4.11	0.70	0.45	4.54	1.54	-	-	<3	0.25	1.17	1.63	-	-	-	-	-	0.64	-	0.68	-	-	-
U	-	-	-	0.86	0.25	0.17	1.01	0.43	-	-	-	0.49	0.66	0.47	-	-	-	-	-	0.23	-	0.27	-	-	-
Cr	176	245	145	172	149	157	176	141	77	223	1100	439	109	50	244	251	208	185	220	173	228	167	51	51	50
Ni	79	137	72	87	157	202	57	88	143	151	406	323	215	27	148	187	137	129	131	149	175	147	58	55	107
Sc	37	34	34	34	47	44	23	29	35	48	37	42	36	34	49	46	50	53	47	43	42	47	33	33	39
V	228	212	226	194	299	266	361	152	289	347	280	215	146	537	336	331	359	372	331	299	311	276	269	266	217
Co	-	-	-	43	50	53	37	54	-	-	63	42	47	43	-	-	-	-	-	49	-	47	-	-	-
Cu	-	-	-	111	90	77	118	40	-	-	100	120	107	398	-	-	-	-	-	86	-	77	-	-	-
Pb	-	-	-	6	5	6	11	5	-	-	10	<5	<5	6	-	-	-	-	-	8	-	<5	-	-	-
Zn	-	-	-	67	113	104	147	147	-	-	77	55	65	143	-	-	-	-	-	93	-	87	-	-	-
La	17.00	15.00	19.00	15.30	4.52	3.75	37.10	19.70	18.00	<3	3.86	2.49	8.81	16.30	<3	<3	<3	<3	3.00	4.60	4.00	5.04	29.00	28.00	16.00
Ce	33.00	35.00	33.00	25.60	10.90	9.00	76.60	41.90	46.00	14.00	8.22	5.93	15.50	38.20	14.00	13.00	13.00	12.00	15.00	10.90	12.00	11.70	68.00	64.00	42.00
Pr	-	-	-	3.59	1.78	1.46	10.50	5.93	-	-	-	0.95	1.94	5.87	-	-	-	-	-	1.75	-	1.82	-	-	-
Nd	18.00	15.00	19.00	14.70	8.91	7.40	45.50	27.50	22.00	11.00	5.26	4.84	7.66	27.90	9.00	9.00	11.00	10.00	10.00	9.04	10.00	9.07	31.00	34.00	17.00
Sm	-	-	-	3.21	2.99	2.38	9.74	6.38	-	-	1.45	1.53	1.63	7.72	-	-	-	-	-	2.81	-	2.94	-	-	-
Eu	-	-	-	1.15	1.15	1.03	3.35	2.26	-	-	0.56	0.73	0.80	2.75	-	-	-	-	-	1.16	-	1.13	-	-	-
Gd	-	-	-	3.83	3.89	3.33	9.68	7.22	-	-	1.86	2.09	1.96	9.26	-	-	-	-	-	3.91	-	3.76	-	-	-
Tb	-	-	-	0.61	0.76	0.63	1.40	1.11	-	-	-	0.40	0.35	1.57	-	-	-	-	-	0.76	-	0.71	-	-	-
Dy	-	-	-	3.84	4.87	4.04	7.52	6.45	-	-	2.67	2.59	2.31	9.18	-	-	-	-	-	4.71	-	4.55	-	-	-
Ho	-	-	-	0.79	1.03	0.86	1.39	1.25	-	-	-	0.54	0.53	1.79	-	-	-	-	-	0.99	-	0.95	-	-	-
Er	-	-	-	2.30	3.11	2.58	3.77	3.56	-	-	1.34	1.62	1.71	5.08	-	-	-	-	-	3.00	-	2.85	-	-	-
Tm	-	-	-	0.36	0.48	0.39	0.49	0.50	-	-	-	0.25	0.28	0.72	-	-	-	-	-	0.46	-	0.42	-	-	-
Yb	-	-	-	2.37	3.06	2.53	3.11	3.24	-	-	1.20	1.59	1.89	4.46	-	-	-	-	-	3.04	-	2.72	-	-	-
Lu	-	-	-	0.33	0.47	0.37	0.37	0.47	-	-	0.18	0.24	0.30	0.61	-	-	-	-	-	0.42	-	0.41	-	-	-
mg#	0.34	0.38	0.34	0.33	0.36	0.36	0.27	0.34	0.29	0.36	0.49	0.44	0.42	0.22	0.39	0.38	0.37	0.36	0.38	0.36	0.37	0.36	0.20	0.18	0.31
FM	0.24	0.27	0.24	0.23	0.30	0.29	0.24	0.31	0.27	0.30	0.42	0.29	0.29	0.26	0.32	0.32	0.31	0.32	0.31	0.29	0.31	0.31	0.25	0.23	0.27

Table 1 - (cont.)

	Metabasite								Amphibolite													
Sample	GO100	GO105	GO106	GO107	GO108	GO110	GO111	GO112	CR03	CR04	CR06	CR10	CR11	CR12	CR105	GO04	GO08	GO01	GO03	GO14	GO15	GO101
SiO_2(%)	49.40	52.20	51.80	49.90	50.20	50.40	50.50	49.50	49.20	49.40	49.70	49.90	52.30	49.40	50.60	49.20	50.70	49.50	49.50	50.30	49.90	52.50
TiO_2	1.71	1.89	1.73	1.00	1.10	0.84	1.02	1.11	1.08	1.39	1.44	1.19	0.25	1.10	0.98	2.13	2.15	2.23	2.06	2.47	2.23	1.87
Al_2O_3	13.77	10.85	11.36	13.05	12.39	12.59	10.35	12.99	12.44	11.96	12.46	12.12	13.43	12.17	12.08	10.19	10.10	9.91	10.45	9.68	10.03	10.49
FeO	13.30	15.96	15.67	11.44	11.67	10.46	11.72	12.11	11.64	12.80	12.80	12.25	9.35	11.95	12.08	17.00	17.37	17.89	16.67	18.04	17.37	15.84
FeOT	13.58	16.30	16.00	11.69	11.91	10.68	11.97	12.37	11.89	13.07	13.07	12.51	9.55	12.20	12.34	17.36	17.74	18.28	17.02	18.43	17.74	16.18
Fe_2O_3	1.79	2.15	2.11	1.54	1.57	1.41	1.58	1.64	1.57	1.73	1.73	1.65	1.26	1.61	1.63	2.29	2.35	2.42	2.25	2.44	2.34	2.14
Fe_2O_3T	15.09	18.11	17.78	12.99	13.24	11.87	13.30	13.75	13.21	14.53	14.53	13.90	10.61	13.56	13.71	19.29	19.72	20.31	18.92	20.48	19.71	17.98
MnO	0.18	0.20	0.19	0.18	0.18	0.18	0.19	0.18	0.19	0.19	0.20	0.19	0.16	0.19	0.19	0.21	0.21	0.22	0.21	0.22	0.22	0.19
MgO	7.24	5.22	5.33	9.34	9.58	10.23	11.79	8.97	10.01	9.11	8.60	9.20	11.83	9.78	9.33	6.36	5.61	5.68	6.21	5.58	5.81	4.97
CaO	9.06	8.65	8.92	11.56	11.45	11.58	9.98	11.21	11.68	11.51	11.09	11.45	9.20	11.74	11.25	10.50	9.60	9.72	10.23	9.59	10.04	8.60
Na_2O	2.69	2.64	2.52	1.67	1.53	1.65	1.46	2.03	1.59	1.77	1.97	1.77	0.82	1.66	1.58	2.19	2.03	2.42	2.59	1.93	2.29	2.93
K_2O	1.09	1.00	1.08	0.24	0.20	0.20	0.23	0.25	0.25	0.23	0.24	0.32	0.04	0.24	0.30	0.73	0.79	0.84	0.71	0.68	0.72	1.18
P_2O_5	0.32	0.33	0.34	0.11	0.10	0.10	0.12	0.14	0.11	0.15	0.15	0.10	0.03	0.11	0.14	0.27	0.30	0.30	0.22	0.30	0.26	0.43
LOI	0.60	0.46	0.64	0.87	1.01	1.15	1.06	0.95	0.99	1.23	0.70	0.88	0.89	0.93	0.84	0.75	0.69	0.91	0.77	1.12	0.97	0.38
Total	100.63	101.18	101.12	100.05	100.03	99.70	98.95	100.19	99.80	100.25	100.39	100.22	98.70	99.95	100.22	101.16	101.26	101.22	101.11	101.29	101.21	101.17
Ba(ppm)	424	346	597	34	55	66	49	53	44	114	53	50	41	65	40	152	146	179	148	220	170	305
Rb	20	22	39	2	7	18	3	2	15	7	7	7	<1	2	4	14	7	22	17	17	20	36
Sr	273	166	204	116	115	113	105	131	114	124	129	124	49	124	114	173	170	110	122	132	160	165
Cs	0.40	0.70	-	<0.1	-	-	-	-	-	0.20	0.10	<0.10	-	-	<0.1	0.20	-	-	-	<0.1	<0.1	-
Ga	20.00	22.00	-	15.00	-	-	-	-	-	19.00	19.00	18.00	-	-	17.00	21.00	-	-	-	22.00	22.00	-
Tl	0.10	0.07	-	<0.05	-	-	-	-	-	0.06	0.08	0.11	-	-	0.07	<0.05	-	-	-	0.07	<0.05	-
Nb	8.60	10.20	10.00	4	4.00	2.00	3.00	2.00	3.00	3.40	3.70	2.30	<2	4.00	2.80	7.00	10.00	10.00	6.00	7.60	7.20	15.00
Zr	153	189	209	57	74	54	75	79	74	79	84	56	10	78	62	197	189	202	159	171	156	312
Ti	10251	11331	10371	5995	6595	5036	6115	6654	6475	8333	8633	7134	1499	6595	5875	12769	12889	13369	12350	14808	13369	11211
Y	30.40	48.60	52.00	19.90	25.00	18.00	20.00	27.00	23.00	26.70	28.10	22.50	12.00	25.00	23.10	39.50	55.00	53.00	44.00	47.00	42.90	60.00
Ta	0.57	0.75	-	1.44	-	-	-	-	-	0.30	0.28	0.17	-	-	0.22	2.74	-	-	-	0.53	0.47	-
Th	2.69	5.00	-	0.46	-	-	-	-	-	0.65	0.73	0.45	-	-	0.53	2.63	-	-	-	2.64	2.38	-
U	0.53	1.27	-	0.17	-	-	-	-	-	0.33	0.37	0.27	-	-	0.23	0.91	-	-	-	0.94	0.81	-
Cr	69	55	61	249	301	393	833	184	359	170	149	195	518	313	233	100	106	102	106	67	86	48
Ni	134	45	51	219	212	267	262	129	202	148	131	94	238	187	326	54	75	81	65	54	72	55
Sc	34	35	36	45	48	48	41	46	45	50	49	52	50	49	45	44	43	40	43	42	42	31
V	238	229	272	261	347	291	277	342	320	292	294	283	234	333	264	259	329	316	327	265	273	256
Co	50	46	-	48	-	-	-	-	-	48	47	43	-	-	62	49	-	-	-	73	56	-
Cu	179	287	-	115	-	-	-	-	-	88	90	54	-	-	60	230	-	-	-	313	343	-
Pb	10	13	-	9	-	-	-	-	-	15	10	9	-	-	6	<5	-	-	-	<5	<5	-
Zn	117	150	-	89	-	-	-	-	-	97	118	97	-	-	121	103	-	-	-	164	186	-
La	19.60	25.30	28.10	3.65	<3	<3	<3	3.00	3.00	4.88	5.38	3.36	<3	<3	4.05	10.70	10.00	10.00	7.00	13.40	11.30	26.00
Ce	37.80	46.20	45.90	8.54	13.00	10.00	10.00	10.00	10.00	11.50	12.40	7.90	<3	12.00	9.40	22.70	34.00	33.00	28.00	28.30	24.70	63.00
Pr	4.99	6.86	-	1.32	-	-	-	-	-	1.85	1.99	1.34	-	-	1.50	3.29	-	-	-	4.04	3.63	-
Nd	21.00	29.40	27.70	6.54	10.00	7.00	8.00	10.00	9.00	9.43	9.73	6.53	<3	8.00	7.81	15.60	22.00	21.00	16.00	19.10	17.30	32.00
Sm	4.80	7.32	6.17	2.15	-	-	-	-	-	2.96	3.06	2.24	-	-	2.36	4.66	-	-	-	5.52	5.01	-
Eu	1.68	2.24	1.96	0.88	-	-	-	-	-	1.13	1.17	0.92	-	-	0.97	1.72	-	-	-	1.93	1.79	-
Gd	5.50	8.85	7.56	2.94	-	-	-	-	-	3.94	3.99	3.02	-	-	3.27	6.06	-	-	-	7.03	6.38	-
Tb	0.93	1.51	-	0.54	-	-	-	-	-	0.72	0.77	0.60	-	-	0.61	1.12	-	-	-	1.33	1.20	-
Dy	5.74	9.20	8.17	3.58	-	-	-	-	-	4.75	4.92	3.91	-	-	4.00	7.12	-	-	-	8.44	7.61	-
Ho	1.16	1.82	-	0.77	-	-	-	-	-	0.98	1.03	0.83	-	-	0.85	1.45	-	-	-	1.76	1.56	-
Er	3.41	5.31	4.37	2.18	-	-	-	-	-	2.97	3.12	2.58	-	-	2.54	4.38	-	-	-	5.16	4.64	-
Tm	0.51	0.80	-	0.35	-	-	-	-	-	0.45	0.47	0.39	-	-	0.39	0.66	-	-	-	0.79	0.69	-
Yb	3.26	4.90	3.54	2.12	-	-	-	-	-	2.81	2.96	2.53	-	-	2.53	4.03	-	-	-	4.85	4.28	-
Lu	0.45	0.68	0.50	0.31	-	-	-	-	-	0.43	0.46	0.38	-	-	0.37	0.62	-	-	-	0.70	0.63	-
mg#	0.30	0.20	0.21	0.39	0.39	0.43	0.44	0.37	0.40	0.36	0.34	0.37	0.50	0.39	0.38	0.23	0.20	0.20	0.22	0.19	0.21	0.20
FM	0.28	0.25	0.25	0.32	0.32	0.33	0.38	0.31	0.34	0.32	0.31	0.32	0.36	0.33	0.32	0.28	0.27	0.27	0.28	0.27	0.27	0.24

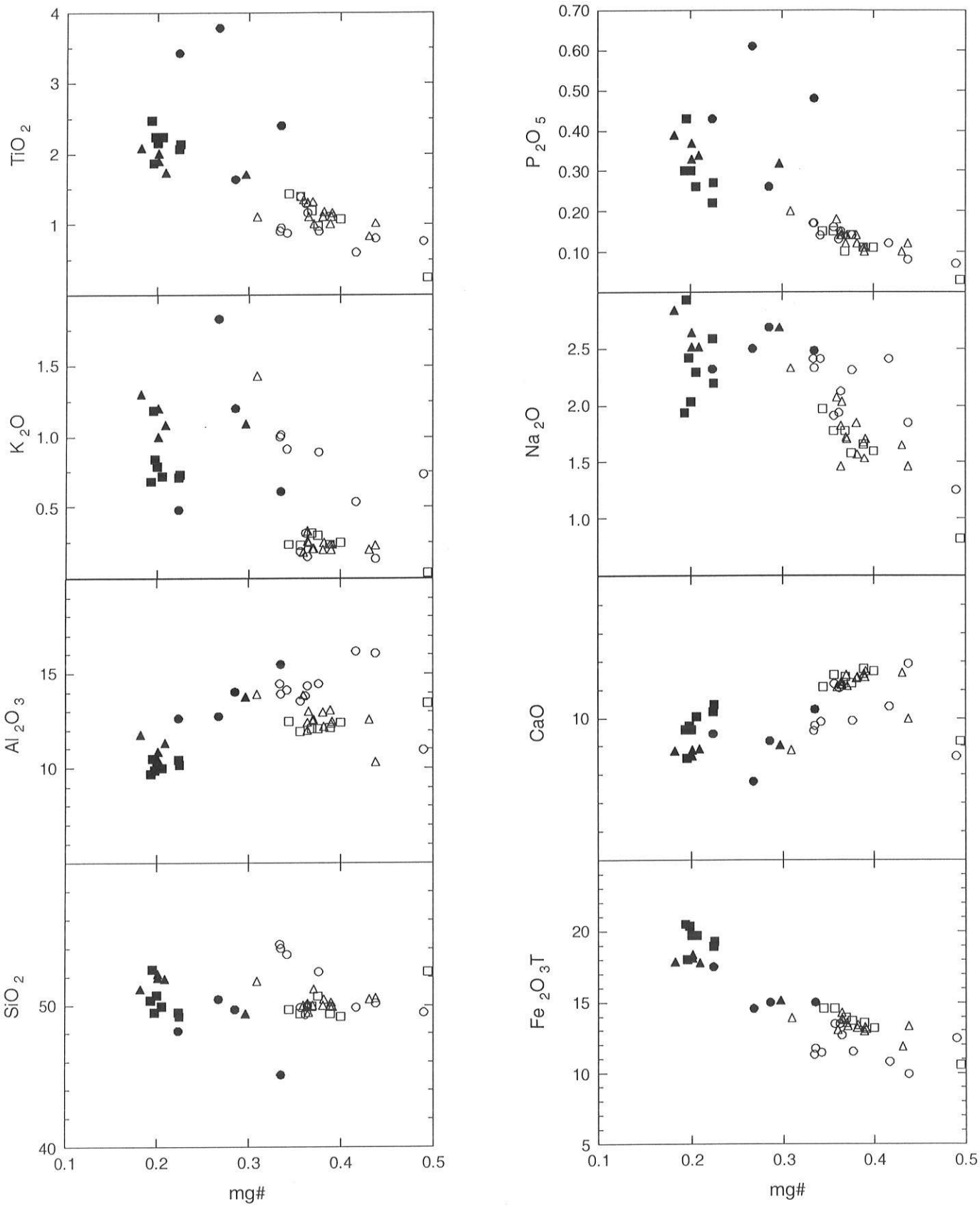

Figure3 - Selected major elements (wt%) vs. mg [molar Mg/ (Mg +Fe_2) ratio: $Fe_2O_3/FeO = 0.15$]. Symbols as in Fig. 2.

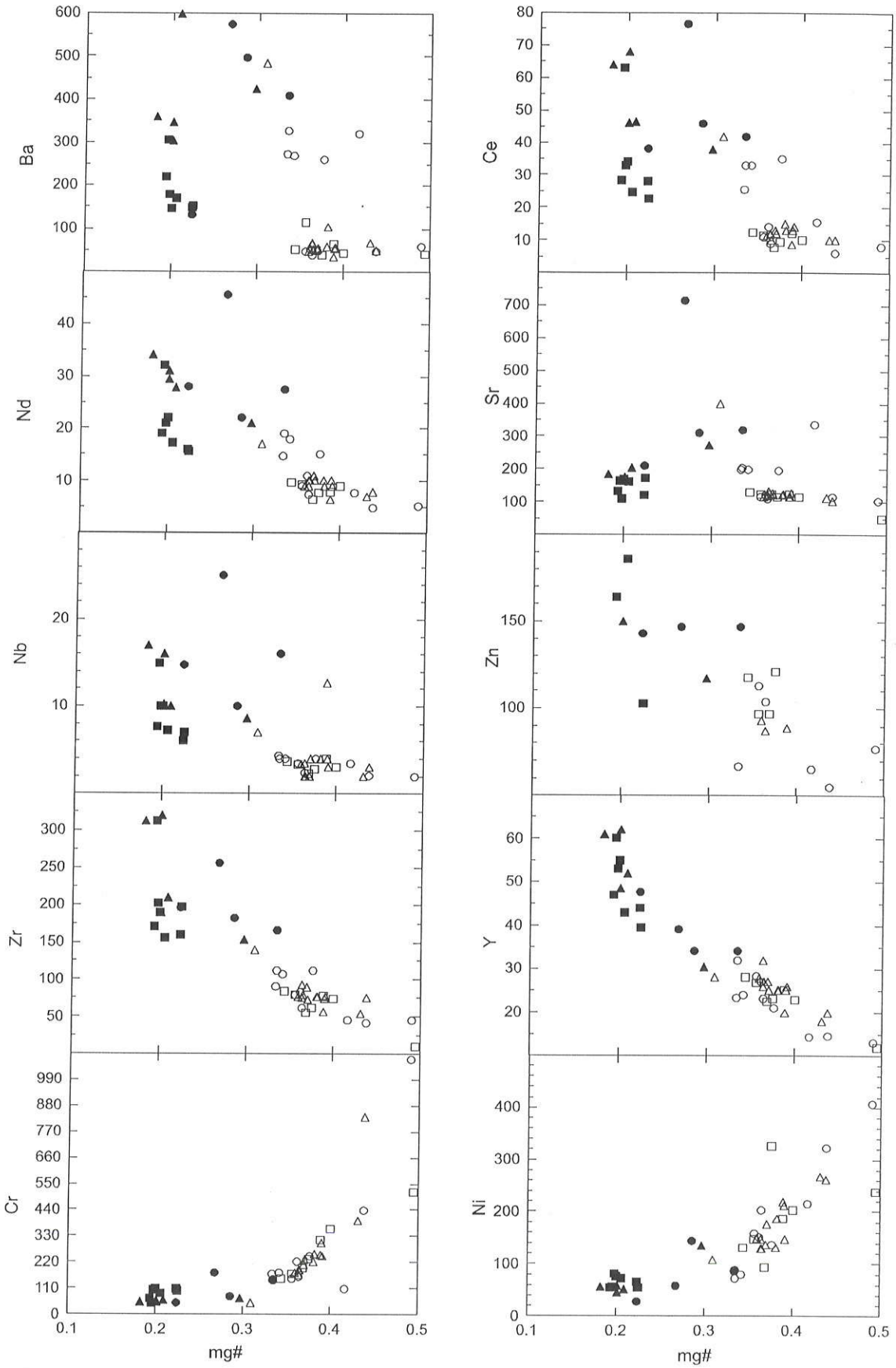

Figure 4 - Selected trace elements (ppm) vs. mg [molar Mg/ (Mg +Fe_2) ratio: $Fe_2O_3/FeO = 0.15$]. Symbols as in Fig. 2.

0.509240–0.509436 (åNd –3.44 to +0.53) in LTi. In HTi Nd_i and åNd values vary from 0.509166 to 0.509340 and from – 4.84 to – 1.7 respectively (Table 3).

å(Sr) versus åNd diagram (Fig. 6) reveals that most of the samples plot near to the " Bulk Earth", varying from fairly depleted to enriched with respect to åSr. In terms of åNd, except for one sample (CR-107), they are slightly depleted. Samples from the basement gneisses, calculated at 2.7 Ga plot close to those of the dykes. The Sr_i and Nd_i values range from 0.70418 to 0.70815 and 0.510942 to 0.510995 respectively.

PETROGENESIS Four petrogenetic processes can theoretically account for the origin of HTi and LTi dykes, i.e. fractional crystallization, crustal contamination, variable degrees of a common

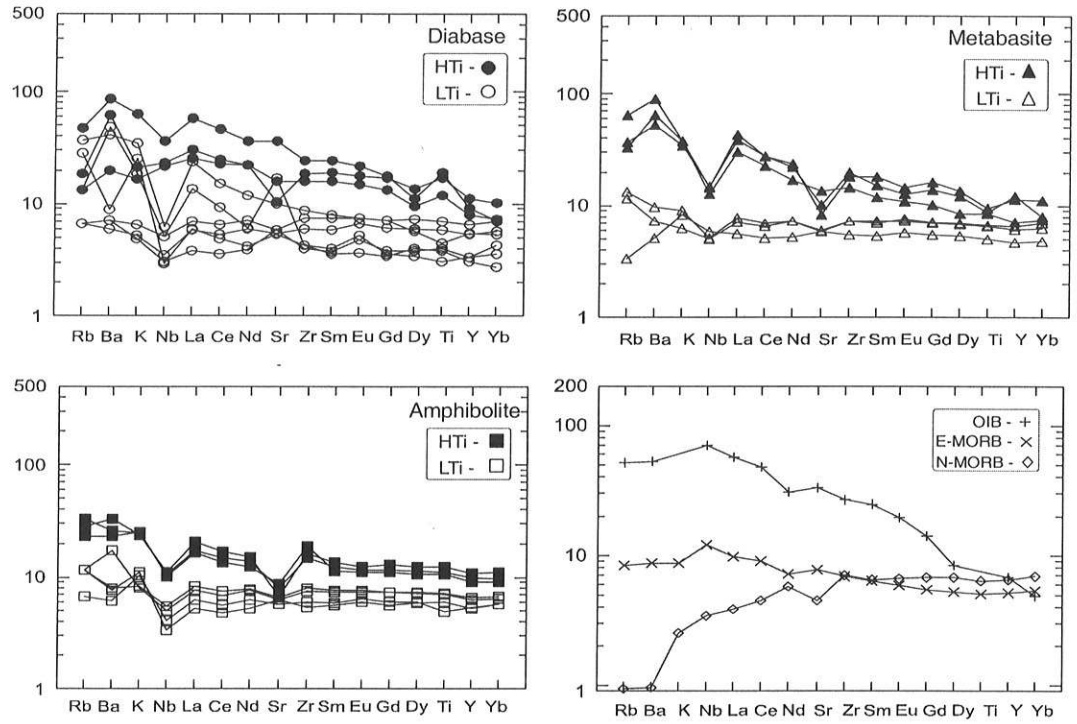

Figure 5 - Multi-elemental plots of diabases, metabasites and amphibolites normalized to primordial mantle of Sun & McDonough (1989). OIB, N-MORB and E-MORB patterns are reported for comparison

Table 2 - Averages and ranges of incompatible trace element ratios of Goiás dykes, compared with N-MORB, E-MORB, OIB and others dyke swarms

	Goiás LTi	Goiás HTi	NMORB	EMORB	OIB	Carajás LTi	Carajás HTi	Salvador LTi	Salvador HTi	Uauá
Rb/Sr	0.08	0.12	0.01	0.03	0.05	0.08	0.12	0.03	0.08	0.10
min-max	0.01-0.16	0.03-0.26								
K/Nb	998.47	727.40	258	253	250	773	451	381	316	402
min-max	415-3030	271-1052								
La/Nb	2.00	1.65	1.10	0.80	0.80	2.15	1.40	1.13	1.07	1.93
min-max	0.91-4.75	1-2.81								
P/Nb	183.70	136.05	219	75	56	143	135	95.82	118	101
min-max	109-305	100-172								
Ti/Zr	90.43	67.08	103	82	61	91	71	102	84	135.3
min-max	47.8-149	35.9-104.9								
Ti/P	11.72	9.05	14.90	9.70	6.40	12.80	9.96	10.70	7.96	12.11
min-max	6.9-16.3	5.9-12.8								
La/Y	0.30	0.43	0.09	0.29	1.28	0.63	0.33	0.36	0.44	0.19
min-max	0.11-0.71	0.16-0.95								
Zr/Y	3.16	4.53	2.60	3.30	9.70	3.9	4.16	3.31	4.45	2.00
min-max	0.83-5.33	3.44-6.55								
Ce/Y	0.63	0.95	0.26	0.68	2.75	1.10	0.85	0.83	1.01	0.50
min-max	0.35-1.67	0.57-1.96								
P/Y	23.82	34.12	18.21	28.18	93.10	—	—	30.59	48.03	19.37
min-max	10.9-36.3	21.8-68.0								
Ti/Y	270	299	271	273	593	246	331	290	340	234
min-max	125-350	187-581								
Ce/Zr	0.18	0.21	0.10	0.21	0.29	0.30	0.18	0.23	0.24	0.25
min-max	0.13-0.34	0.12-0.30								

Table 3 - Rb/Sr, Sm/Nd ratios, $(^{87}Sr/^{86}Sr)_i$, $(^{143}Nd/^{144}Nd)_i$, εSr and εNd of the Goiás dykes (assumed age 2.49 Ga) and of basement gneisses (assumed age 2.7 Ga). Isotopic data of gneisses after Pimentel et al. (1996, 2003).

Diabase						
Sample	Rb/Sr	Sm/Nd	$(^{87}Sr/^{86}Sr)i$	$(^{143}Nd/^{144}Nd)$	ε(Sr)	ε(Nd)
CR-01/LTi	0.4419	0.1373	0.70049	0.509300	-15.24	-2.28
CR-102/LTi	0.3771	0.1370	0.70306	0.509240	21.39	-3.44
CR-103/LTi	0.1252	0.1986	0.70134	0.509347	-3.17	-1.21
CR-107/Lti	0.1015	0.1945	0.70116	0.509436	-5.78	0.53
GO-06/Lti	0.2235	0.1985	0.70047	0.509377	-15.50	-0.66
GO-07/LTi	0.4165	0.1799	0.70003	0.509244	-21.89	-3.25
GO-104/LTI	0.0941	0.1988	0.70065	0.509389	-12.96	-0.38
Metabasite						
Sample	Rb/Sr	Sm/Nd	$(^{87}Sr/^{86}Sr)i$	$(^{143}Nd/^{144}Nd)$	ε(Sr)	ε(Nd)
CR-104/lti	0.1156	0.1956	0.70132	0.509402	-3.50	-0.14
CR-108/LTi	0.2159	0.1898	0.70179	0.509372	3.28	-0.73
GO-105/HTi	0.4379	0.1573	0.70483	0.509166	46.52	-4.84
GO-107/LTi	0.0601	0.1960	0.70405	0.509357	35.39	-1.01
Amphibolite						
Sample	Rb/Sr	Sm/Nd	$(^{87}Sr/^{86}Sr)i$	$(^{143}Nd/^{144}Nd)$	ε(Sr)	ε(Nd)
CR-04/LTi	0.1969	0.1913	0.70029	0.509357	-18.17	-1.02
CR-10/LTi	0.1797	0.2082	0.70283	0.509180	18.05	-4.42
CR-105/lti	0.1098	0.1929	0.70256	0.509371	14.24	-0.75
GO-01/HTI	0.4472	0.1840	0.70314	0.509340	22.55	-1.37
Basement Gneiss						
Sample	Rb/Sr	Sm/Nd	$(^{87}Sr/^{86}Sr)i$	$(^{143}Nd/^{144}Nd)$	ε(Sr)	ε(Nd)
MP581I	0.1586	0.1148	0.70815	0.510942	10.75	-5.93
MP581F	0.0814	0.1101	0.70467	0.510963	2.54	-3.97
MP581B	0.0393	0.1237	0.70418	0.510995	18.11	-7.84

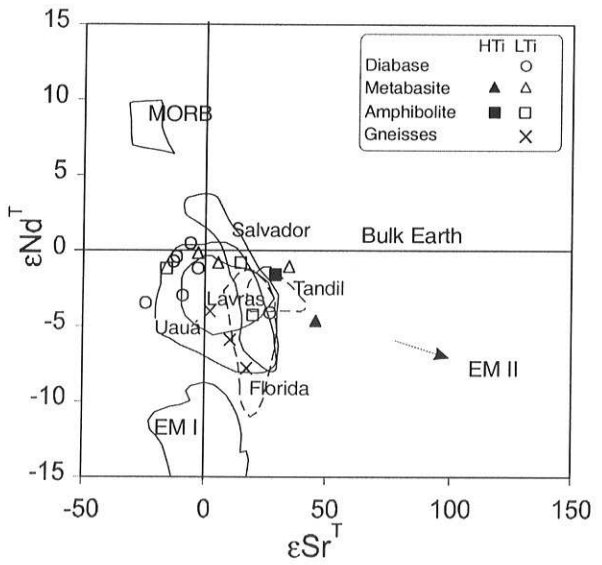

Figure 6 - εSr vs. εNd diagram for 2.49 Ga Goiás dykes. 2.7 Ga basement gneisses (Pimentel et al. 1996, 2003), fields from the São Francisco (Uauá 2.2-2.0 Ga, Bastos Leal et al. 1994, Salvador 1.2-1.0 Ga, Bellieni et al. 1998, Lavras 1.9 Ga, Pinese 1997) and Rio da Plata Cratons (Florida 1.7 Ga, Mazzucchelli et al. 1995, Tandil 1.6 Ga, Iacumin et al. 2001) are reported for comparison. MORB, EMI, EMII after Zindler & Hart (1986).

source material and mantle heterogeneity. These mechanisms will be discussed on the basis of geochemical and isotopic data.

Fractional crystallization We tested crystal fractionation by using mass balance calculations using the Genesis softwar (Teixeira 1997), which is adapted from the XLFRAC program (Stormer & Nicholls 1978). Average chemical compositions of clino and orthopyroxenes, plagioclase, amphibole, magnetite and ilmenite (Corrêa da Costa & Girardi 2004) were used in order to perform fractional calculations. Olivine composition was calculated after Bellieni et al. (1995). A Rayleigh fractionation model was tested to compare calculated and observed trace elements contents. The crystal fractionation is modelled by:

$$C_L = C_O \cdot F^{(D-1)}$$

where C_L is the concentration of a trace element in the residual liquid., C_O is the concentration of the trace element in the initial liquid,. D is the bulk distribution coefficient of the element and F the liquid fraction remaining after the fractionation.

Figure 7 displays several calculated crystal fractionation trends, either testing the derivation of HTi from the LTi suite, or checking the relationship between samples of the same group. The transition from the less evolved basaltic melt (sample GO 07, mg# 0.49) to dykes which average mg# values is 0.36 (AV-2: samples CR 107, CR 103 and GO 06) is compatible with 32% removal of olivine (8%), orthopyroxene (14%), augite (5%) and

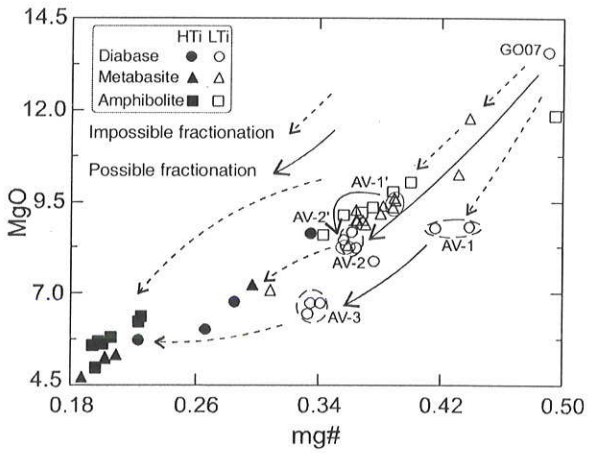

Figure. 7 - Possible and impossible fractional crystallization trends. See text for sample numbers

Table 4 - Mass balance calculations for fractional crystallization transition from less (GO-07) to the mean of mg# 0.36 dykes (AV-2). Ol - olivine, Opx – orthopyroxene, Aug – augite, Pl – plagioclase, Calc. calculated, Obs. observed, AV average, åres2 sum of squares of major residual elements, SR % of removed solid fraction.

	GO07	AV-2			Ol	Opx	Aug	Pl
	(obs.)	(obs.)	(calc.)	calc./obs.				
SiO_2(%)	49.50	49.70	49.38	0.99	39.30	55.26	51.83	50.93
TiO_2	0.76	1.28	1.13	0.88	0	0.10	0.37	0.02
Al_2O_3	10.96	13.90	13.61	0.98	0	1.36	3.39	31.47
Fe_2O_3T	12.43	13.21	13.08	0.99	17.03	11.22	7.88	0.83
MnO	0.18	0.18	0.19	1.06	0.30	0.25	0.19	0
MgO	13.58	8.45	8.76	1.04	43.00	29.53	17.18	0
CaO	8.66	11.15	10.93	0.98	0.37	2.25	18.91	13.04
Na_2O	1.25	1.99	1.70	0.85	0	0.04	0.25	3.39
K_2O	0.73	0.22	0.98	4.45	0	0	0	0.32
P_2O_5	0.07	0.15	0.10	0.67	0	0	0	0
SR					7.8	14.2	4.9	5.0
$\sum res^2$	0.45							
Cr	1100	176	185	1.05				
Ni	406	170	137	0.81				
Sr	105	115	138	1.20				
Nb	2	3	2.86	0.95				
Zr	45	75	63.52	0.85				
Y	13	26	17.51	0.67				
La	3.86	4.14	5.59	1.35				
Ce	8.22	11.3	11.90	1.05				
Nd	5.26	9.1	7.55	0.83				
Sm	1.45	2.69	2.03	0.75				
Gd	1.86	3.61	2.54	0.70				
Dy	2.67	4.46	3.59	0.80				

Table 5 - Mass balance calculations for fractional crystallization transition from 0.42-0.44 mg# (AV-1) to 0.33-0.34 mg# dykes (AV-3). Others abbreviations and notations as in Table 4.

	AV-1	AV-3			Ol	Opx	Aug	Pl	Mt	ilm
	(obs.)	(obs.)	(calc.)	calc./obs						
SiO_2(%)	49.95	53.95	53.30	0.99	39.30	55.26	51.83	50.93	0.09	0.07
TiO_2	0.71	0.91	0.87	0.96	0	0.10	0.37	0.02	0.78	51.37
Al_2O_3	16.13	14.19	14.25	1.00	0	1.36	3.39	31.47	0.42	0.03
Fe_2O_3T	10.42	11.52	11.35	0.99	17.03	11.22	7.88	0.83	98.66	47.24
MnO	0.17	0.17	0.20	1.18	0.30	0.25	0.19	0	0.01	0.71
MgO	8.80	6.62	6.76	1.02	43.00	29.53	17.18	0	0.04	0.43
CaO	11.17	9.73	9.79	1.01	0.37	2.25	18.91	13.04	0	0.15
Na_2O	2.13	2.38	2.56	1.08	0	0.04	0.25	3.39	0	0
K_2O	0.34	0.97	0.70	0.72	0	0	0	0.32	0	0
P_2O_5	0.10	0.16	0.25	1.56	0	0	0	0	0	0
SR					5.5	4.1	17.0	32.3	2.6	0.5
$\sum res^2$	0.029									
Cr	274	164	19.08	0.12						
Ni	269	79	128	1.62						
Sr	226	199	234	1.18						
Nb	3.0	4	7.63	1.91						
Zr	44	103	108	1.05						
Y	14	26	27.94	1.07						
La	5.65	17.1	13.24	0.77						
Ce	10.72	30.53	25.47	0.83						
Nd	6.25	17.23	14.48	0.84						
Sm	1.58	3.21	3.43	1.07						
Gd	2.03	3.83	4.08	1.07						
Dy	2.45	3.84	4.89	1.27						

plagioclase (5%). Table 4 shows the difference between observed and calculated major and trace element contents.

Two other possible differentiation trends were tested by assuming initial melts with average mg# values varying from 0.42 to 0.44 (AV- 1; GO 104 and GO 109). This melt can produce rocks with average mg# compositions from 0.33 to 0.34 (AV 3: CR1, CR 101 and CR 102) by a 54% extraction of olivine (6%), orthopyroxene (4%), augite (17%), plagioclase (32%) and magnetite plus ilmenite (3%) (Table 5). The other possibility is to produce, from the same initial melt, rocks with average mg # 0.36, by 51% removal of orthopyroxene (10%), augite (7%), plagioclase (28%), amphibole (5%) and magnetite (1%) (Table 6).

These calculations indicate that fractional crystallization can be an effective mechanism of magma evolution within the domains of the different studied rock suites (LTi and HTi). Moreover, differentiation seems to have originated from several parental melts, which is supported by important differences in incompatible element contents (e.g. Zr, Y, Ce, La) for similar mg# values (Table 1). Crystal fractionation calculations demonstrate, however, that the origin of HTi and LTi suites cannot be attributed to the same parental magmas.

Crustal contamination Crustal contamination was tested by using the ACF model (De Paolo 1981), which implies that contamination and fractional crystallization are simultaneous processes in the magma chamber, and by diagrams using Sr_i and typical crustal elements. Both plots indicate that crustal contamination did not play an important role, because there is no positive

Table 6 - Mass balance calculations for fractional crystallization transition from 0.42-0.44 mg# (AV-1) to 0.36 mg# dykes (AV-2). Others abbreviations and notations as in Table 4.

	AV-1	AV-2'			Opx	Aug	Pl	Anf	Mt
	(obs.)	(obs.)	(calc.)	calc./obs.					
SiO_2(%)	49.95	50.05	49.88	1.00	55.26	51.83	50.93	43.39	0.09
TiO_2	0.71	1.33	1.10	0.83	0.10	0.37	0.02	2.71	0.78
Al_2O_3	16.13	13.15	13.18	1.00	1.36	3.39	31.47	10.55	0.42
Fe_2O_3T	10.42	13.43	13.21	0.98	11.22	7.88	0.83	19.47	98.66
MnO	0.17	0.19	0.24	1.26	0.25	0.19	0	0.23	0.01
MgO	8.80	8.64	8.58	0.99	29.53	17.18	0	9.90	0.04
CaO	11.17	11.13	11.06	0.99	2.25	18.91	13.04	10.80	0
Na_2O	2.13	1.95	2.12	1.09	0.04	0.25	3.39	2.36	0
K_2O	0.34	0.22	0.45	1.86	0	0	0.32	0.60	0
P_2O_5	0.10	0.17	0.20	1.18	0	0	0	0	0
SR					9.9	7.2	28.3	4.6	1.1
$\sum res^2$	0.038								
Cr	274	170	20.83	0.12					
Ni	269	148	124	0.84					
Sr	226	117	222	1.90					
Nb	3.0	3	5.86	1.95					
Zr	44	77	83.32	1.08					
Y	14	27	24.06	0.89					
La	5.65	4.82	10.65	2.21					
Ce	10.72	11.3	20.43	1.81					
Nd	6.25	9.06	11.71	1.29					
Sm	1.58	2.88	2.85	0.99					
Gd	2.03	3.84	3.25	0.85					
Dy	2.45	4.63	3.77	0.81					

correlation between Sr_i and crustal elements (Rb, SiO_2, K_2O, Sr) or ratios (Rb/Sr and La/Yb). Moreover, Sr_i of the dykes is < 0.705, and the values of Sr_i, εSr and εNd of the possible contaminants (the basement gneisses) are two low to cause obvious contamination (Table 3, Fig. 6).

Variable degrees of melting of a common source material Different degrees of melting from a homogeneous source could also explain the existence of HTi and LTi suites. However, the large difference between incompatible elements ratios hampers the possibility. HTi incompatible ratios are approximately 1.5 times larger than LTi values (Fig. 8). In order to derivate both suites from an homogeneous source, it would be necessary to admit 1% to 2% mantle melting to give rise to HTi (e.g. Bellieni et al. 1984, Correia & Girardi 1989). Such melting degrees are incompatible with generation of tholeiitic magmas, which demand 15-25% melting (Kushiro 2001). The trace elements patterns of the dykes are compared with model melts that experienced 50% of crystal fractionation, assuming relative proportions of olivine (20%), clinopyroxene (50%) and of plagioclase (30%). The melting degrees correspond to 10, 15, 25 and 30% of non-modal batch melt of a primitive source (Mc Donough & Sun 1995), in garnet and spinel peridotite facies (Fig. 9 and 10). Fractional and melting models were carried out according to partition coefficients reported by Bossi et al. (1993).

The assumed mineralogical compositions of the garnet and spinel facies peridotites are respectively: olivine (60 and 51%), orthopyroxene (25 and 20%), clinopyroxene (10 and 23%), garnet (5%), in garnet facies, and spinel (6%), in spinel facies mantle. Both models admit the generation of LTi by 15 to 30% of mantle melting. However the origin of HTi from the same source would imply in less than 10% melting, which is incompatible with the composition of tholeiitic melts (Kushiro 2001).

Mantle heterogeneity Mantle heterogeneity has been discussed by many authors (e.g. Faure & Hurley 1963, Weaver 1991, Dickin 1997, Reiners 2002). Studies carried out on the mafic dyke swarms in South America (e.g. Bellieni *et al.* 1995, Mazzucchelli *et al.* 1995, Menezes Leal *et al.* 1995, Girardi *et al.* 1996, Rivalenti *et al.* 1998) indicate that these intrusions originated from heterogeneous mantle sources under the various cratons of the South American Platform. The mechanism seems to be effective both in large areas, as shown by the basalts of the Paraná Basin (Bellieni *et al.* 1984), and also in smaller regions (Correia & Girardi 1989).

The variable chemical composition of original basaltic melts produced in several environments, such as continental tholeiites, oceanic islands basalts (OIB) and island arc basalts (IAB) can be explained by mixtures of several geochemical components (HIMU, EMI, EMII) and the depleted mantle (DMM). HIMU and EMII are generally accepted as derived from subducted oceanic crust and continental sediments respectively (Dickin 1997). The origin of EMI is debatable, either resultant from mantle metasomatism (Hart 1988), from contamination by pelagic sediments (Weaver 1991), or from subducted sub-continental lithosphere from craton margins (Tatsumoto & Nakamura 1991).

The origin of mantle heterogeneity is, however, a controversial matter. One hypothesis attributes the metasomatic enrichment of the lithospheric mantle to the interaction with plumes, either with large up to 2000 km heads, which started in the asthenosphere, or smaller ones, from shallower sources (e.g. Saunders *et al.* 1992, Condie 2001). King & Anderson (1998) and Anderson (2003) criticize the plume model. According to Anderson (2003),

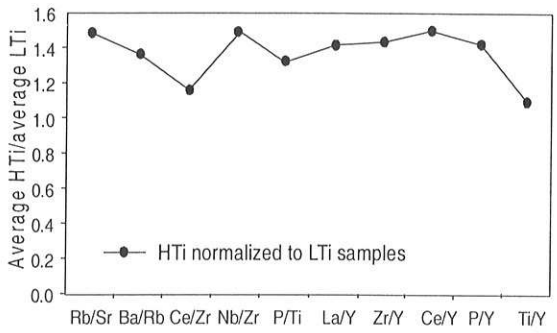

Figure 8- Average incompatible element ratios normalized to average LTi samples.

geophysical measurements, mantle temperatures and other evidences are against the plume hypothesis. King & Anderson (1998) propose that convection currents originated at the boundary between thick and thin lithosphere are responsible for small-scale flows, which drive the ascent of the melting material (edge-driven convection). Sheraton & Black (1981) and Ellam & Cox (1989) advocate non-subduction related metasomatism of the lithospheric mantle caused by mantle fluids or melts from deeper mantle.

Based on seismologic and geochemical data, Helffrinch & Wood (2001) propose that the observed mantle heterogeneities are remnants of recycled continental and oceanic crust that make up respectively about 0.3 and 16% of the mantle volume. According to these authors, fragments of variable ages and sizes of oceanic and continental crust dispersed in a sterile highly depleted peridotite constitute the mantle. This simple model is consistent with variable scale heterogeneity. This article and many others (e.g. Weaver *et al.* 1987, Hergt *et al.* 1991, Zhao & McCulloch 1993) advocate contamination by ancient subducted crustal material as the most acceptable mechanism to explain mantle heterogeneity, which has been proposed for arc and cratonic areas. The role of eclogites from subducted slabs on the origin of basaltic rocks has been emphasized in many papers (e.g. Cordery *et al.* 1997, Takahashi *et al.* 1998, Ayers 1998, Rivalenti *et al.* 1998, Leitch & Davis 2001). The metasomatic effects caused by small melts or/ and fluids derived from trapped eclogites on depleted mantle peridotites give rise to a mixed source accountable for the basaltic melts. Several papers (Rapp *et al.* 1991, Brenan *et al.* 1994, Ayers 1998) demonstrate that rutile is a residual phase from eclogite melts or fluids. According to the experiments, rutile/fluid partition coefficients have high Nb, intermediate REE, and low Rb and Sr values. Small amounts of rutile (~2%) are enough to prevent HSFE enrichment in the mantle wedge (Brenan *et al.* 1994). Consequently, magmas originated from the proposed mixed source have high LILE/ HSFE and REEE/HSFE ratios. The retention of Y in eclogite garnets accounts for high LREE/HREE ratios.

The model proposed by Rivalenti *et al.* (1998) to justify the presence of LTi and HTi tholeiites in the Carajás region is based on the presence of a continental mantle containing veins and lenses of eclogite. LTi basalts derive from peridotites metasomatised by acid melts produced by incipient melting of eclogites. HTi basalts are produced by melting of peridotites containing the complementary residual eclogites.

According to Ayers (1998) the interaction between fluids from eclogites in the subducted slab and depleted peridotites produces a mixed source. This model emphasizes the amount of wedge

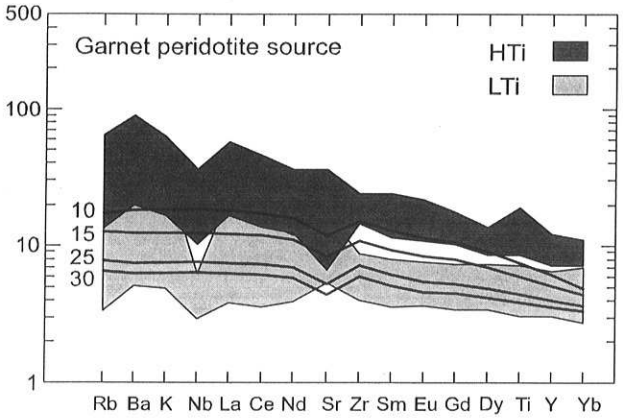

Figure. 9 - Incompatible trace-element variation patterns normalized to primordial mantle (Sun and McDonough 1989) of HTi and LTi dykes. The lines labelled 10, 15, 25 and 30% are the result of 50% fractionation (ol 20, cpx 50 and pl 30) of a primitive model melts derived by non-modal batch melting of primitive garnet peridotite source (McDonough & Sun 1995) Partition coefficients after Bossi et al. (1993).

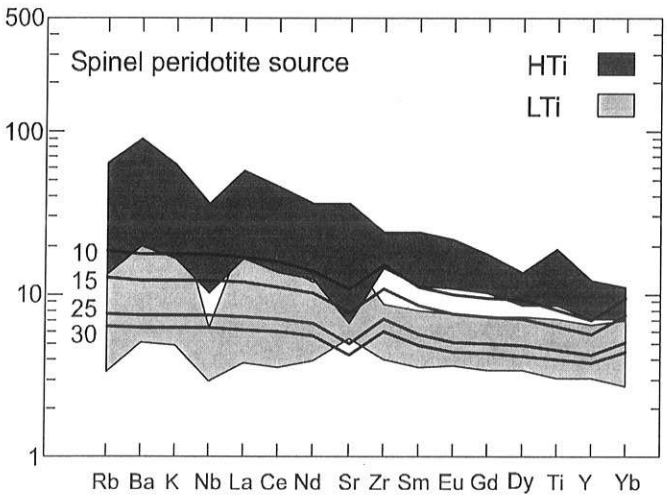

Figure 10 - Incompatible trace-element variation patterns normalized to primordial mantle (Sun and McDonough 1989) of HTi and LTi dykes. The primitive source is spinel peridotite. Other notations and abbreviations as Fig. 9.

peridotite processed by the fluids. The concentration of IE increases as fluid processes the peridotites in the wedge, due to their lower compatibility in the wedge with respect to the slab. Consequently it is possible to originate variable sources in terms of enrichment, which account for different trace element signature of the originated melts. The origin of tholeiites with distinct IE concentrations is compatible with the model.

Mantle heterogeneity is the only possible process to explain the origin of LTi and HTi dykes of the studied area. A possible mechanism responsible for the origin of the heterogeneous mantle source will be discussed on the basis of geochemical, isotopic and geologic data.

GEOTECTONIC SETTING AND CONCLUDING REMARKS

To deduce evidences for the possible geotectonic setting of the Goiás swarm, geochemical and isotopic data of the studied dykes are compared to basaltic rocks of several geological environments. Figure 11 displays the comparison among IE patterns of the Goiás LTi and HTi tholeiites and other basaltic suites. The compositional fields of the Goiás and Carajás dykes, which intrude the Amazonic Craton, are very similar. The main differences are due to the larger Nb anomaly in Goiás, and the Sr spike in both HTi suites, which is positive in Goiás and negative in Carajás. The fields defining the composition of the Goiás, Salvador and Uauá swarms, in the São Francisco Craton, are also similar, despite some differences in Nb, Zr and Sr anomalies. When compared to the Mesozoic basalts of the Paraná Basin, the Goiás swarm displays less enriched patterns. Table 2 exhibits incompatible element ratios of HTi and LTi dykes of Goiás and those of the intracratonic Proterozoic dyke swarms of the São Francisco and Amazonic Cratons. Almost all HTi and LTI ratios of the Goiás dykes are similar to those of Carajás, and most of them similar to the Salvador dykes. The ratios of the Uauá swarm are closer to those of the LTI Goiás bodies. The most important difference between the incompatible element ratios of these swarms is the conspicuous Nb negative spike in Goiás, which is responsible for the higher LILE/Nb and LREE/Nb ratios in both LTi and HTi suites (e.g. La/ Nb and K/Nb in Table 2).

Figure 6 displays εSr and εNd values of the Goiás and other Proterozoic dyke swarms of the South American Platform. The isotopic signature of the Goiás dykes is similar to those from the São Francisco Craton (Uauá, Salvador and Lavras). The dykes from the Rio da Plata Craton are slightly different. The Tandil tholeiites, Argentina (Iacumin *et al.* 2001), have higher εSr; and the Florida swarm, Uruguay (Mazzuchelli *et al.* 1995), is more enriched in the EMI component.

The similarities between the geochemical and isotopic characteristics of the Goiás and other Proterozoic intracratonic tholeiitic swarms, mainly those of the São Francisco (Menezes Leal *et al.* 1995, Bellieni *et al.* 1995, 1998, Pinese 1997) and Amazonic (Rivalenti *et al.* 1998) Cratons, suggest a similar geologic setting.

Available geochemical and isotopic data constrain the mantle source composition of the Goiás swarm. The εSr versus εNd diagram shows that the majority of samples plot near "Bulk Earth". Sr_i values range from 0.700 to 0.705 (εSr = -21.89 to 46.52). Nd_i varies from 0.5092 to 0.5120 (εNd -4.84 to +0.53) (Fig. 6 and Table 3). These values suggest that the parental mantle is composed by a DMM end-member enriched by another component. The scatter of εSr values renders difficult the determination of a clear trend toward other possible end-members (EMI or EMII). However the plots are close to EMI and the εSr- εNd field of Goiás is similar to those of Uauá, Lavras and Tandil swarms, whose signatures are considered to have an EMI component (Iacumin *et al.* 2001). Moreover, according to Iacumin et al. (2003), Precambrian tholeiites of the South American Platform in general trend towards EMI. These observations indicate that the EMI component is the other most probable end-member of the mantle source of the Goiás dykes IE patterns display two distinct levels of enrichment corresponding to two parental sources. HTi dykes exhibit patterns broadly intermediate between E-MORB and OIB, whereas LTi patterns display general characteristics of E-MORB and some of N-MORB. However these patterns have also characteristic features of IAB and continental basalts, as shown by the pronounced negative anomaly of Nb relative to LREE and LILE, which indicates retention of HSFE in the source both in LTi and HTi suites. Isotopic data

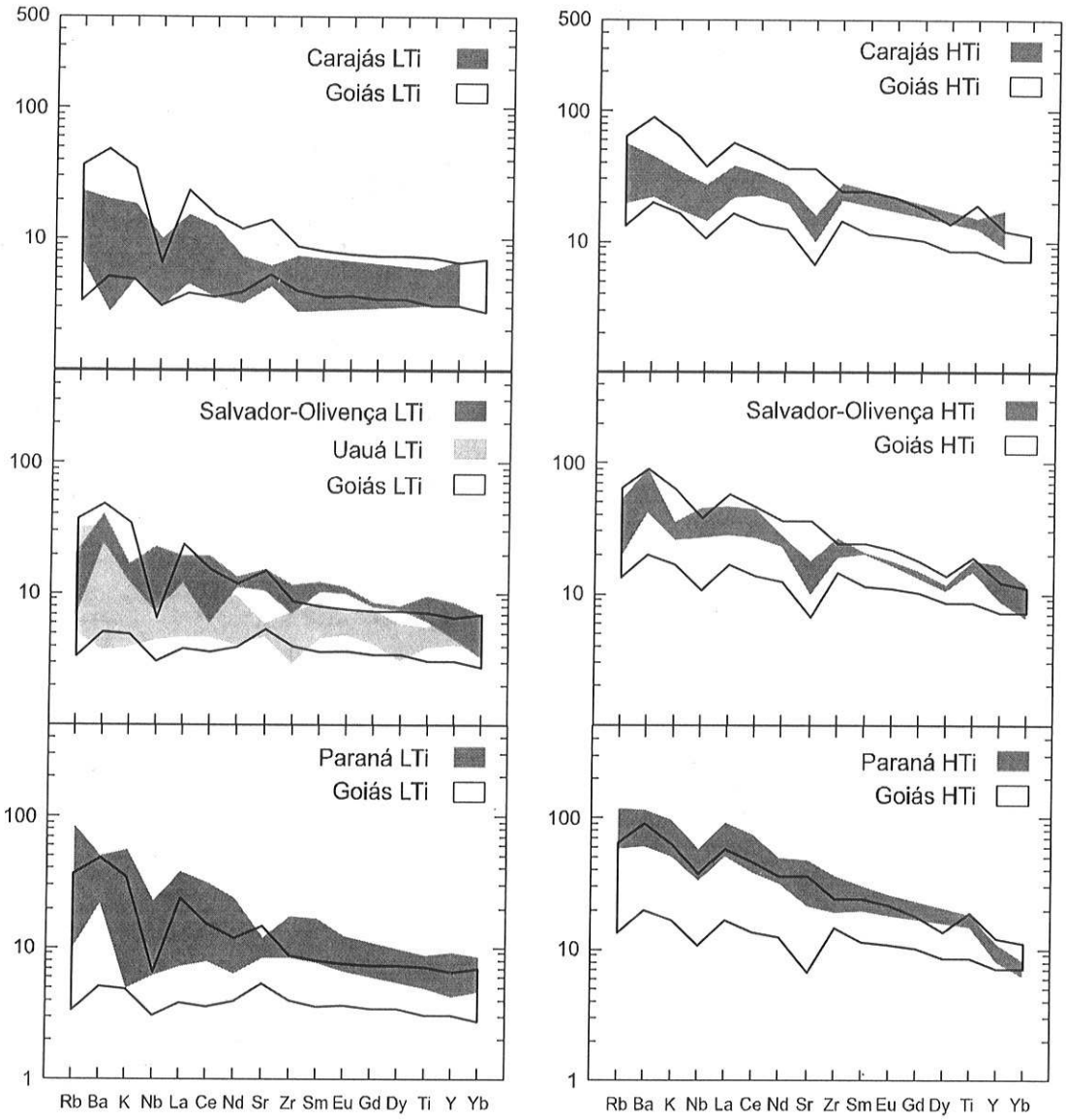

Figure 11- Comparison among multi-elemental diagrams, normalized to the primordial mantle (Sun & McDonough 1989) of dykes of Goiás, Carajás (Amazonic Craton), Salvador and Uauá (São Francisco Craton), and the Paraná basalts.

suggest an EMI component added to the depleted mantle. These features are compatible with a source originated from the mixture of a depleted mantle and oceanic subducted slab. Metasomatic fluids and/or small volume melts derived from slab eclogites gave rise to the higher and lower IE concentrations, which characterize the HTi and LTi dykes respectively, according to models of Ayers (1998) and Rivalenti *et al.* (1998). Depletion in Nb accounts on the retention by rutile of eclogites. Positive Ba anomalies of HTi originate probably from pelagic sediments associated within the slab.

The origin of the Archean Block of the Goiás Massif is controversial. It is a cratonic fragment, which was probably either a microcontinent, or part of the border of the São Francisco or the Amazonic Craton (Brito Neves et al. 1999, Campos Neto 2000, Correia 2001) untill the Statherian (1.6-1.8 Ga). The Goiás dykes intruded in the Archean 2.71-2.94 Ga gneisses of the Goiás Block at approximately 2.49 Ga. Consequently the subduction of the oceanic crust under the cratonic Archean Block of Goiás-Crixás must have occurred during Archean-Paleoproterozoic times. According to Iacumin *et al.* (2003) ancient subduction, related metasomatism, and consequent mantle heterogeneity processes played an important role on the origin of South American tholeiites. Several swarms of the South American Platform are Paleoproterozoic, yielding ages up to 2.49 Ga (e.g. Bastos Leal *et al.* 1994, Menezes Leal *et al.*1995, Teixeira 1990, Teixeira *et al.* 1999, Bellieni *et al.* 1995, Tomazzoli 1997, Pinese 1997, Corrêa da Costa 2003), which indicates that subduction was an important geotectonic process in the South American Platform since the Archean.

Acknowledgments The authors acknowledge FAPESP and CNPq for financial support. We are also grateful to Y. MacReath for reviewing the manuscript, and to RBG reviewers for suggestions to the manuscript.

References

Anderson D.L. 2003. Look again. *Geophys. Res. Let.*, **1**:10-11.

Ayers J.1998. Trace element modeling of aqueous fluid-peridotite interaction in the mantle wedge of subduction zones. *Contr. Mineral. Petrol.*, **132**:390-404.

Bastos Leal L.R., Teixeira W., Piccirilo E.M., Menezes Leal A.B., Girardi V.A.V. 1994. Geocronologia Rb/Sr e K/Ar do enxame de diques máficos de Uauá, Bahia (Brasil). *Geochim. Bras.*, **8**:99-114.

Bellieni G., Comin Chiaramonti P., Marques L.S., Melfi A.J., Piccirillo E.M., Nardy A.J.R., Roisenberg A. 1984. High- and low- TiO_2 flood basalts from the Paraná plateau (Brazil): petrology and geochemical aspects bearing on their mantle origin. *Neues Jahrbuch Miner. Abh.*, **150**:273-306.

Bellieni G., Petrini R., Piccirillo E.M., Cavazzini G., Civetta L., Comin Chiaramonti P., Melfi A.J., Bertolo S., De Min A. 1991. Proterozoic mafic dyke swarms of the Sao Francisco Craton (SE-Bahia State, Brasil): petrology and Sr-Nd isotopes. *Eur. Journ. Mineral.*, **3**:429-449.

Bellieni G., Piccirillo E.M., Petrini R., Girardi V.A.V., Menezes Leal A.B., Teixeira W., Bastos Leal L.R., De Min A., Comin Chiaramonti P., Tanner de Oliveira M.A.F. 1995. Petrological and Sr-Nd evidence bearing on Early Proterozoic magmatic events of the subcontinental mantle: São Francisco Craton (Uauá, NE-Brasil). *Contr. Mineral. Petrol.*, **122**:252-261.

Bellieni G., Petrini R., Piccirillo E.M., Brito C.M., Figueiredo A.M.G., Marques L.S., De Min A., Melfi A.J. 1998. Petrogenesis and tectonic significance of the Late Proterozoic unmetamorphosed mafic dyke swarms from the Salvador area (NE Brazil). *Neues Jahrbuch Miner. Abh.*, **173**:327-350.

Beswick A.E. 1982. Some geochemical aspects of alteration and genetic relations in komatiitic suites. **In:** N.T. Arndt & E.G. Nesbitt (Eds.) *Komatiites*. London, George Allen and Unwin: 283-308.

Bossi J., Campal N., Civetta L., Demarchi G., Girardi V.A.V., Mazzucchelli M., Negrini L., Rivalenti G., Fragoso Cesar A.R.S., Sinigoi S., Teixeira W., Piccirillo E.M., Molesini M. 1993. Early Proterozoic dike swarms from western Uruguay: geochemistry, Sr-Nd isotopes and petrogenesis. *Chemical Geology*, **106**:263-277.

Brito Neves B.B., Campos Neto M.da C., Fuck R.A. 1999. From Rodinia to Western Gondwana: An approach to the Brasiliano-Pan African Cycle and orogenic collage. *Episodes*, **22**:155-166.

Brenan J.M., Shaw H.F., Phinney D.L., Ryerson F.J. 1994. Rutile-aqueous partitioning of Nb, Ta, Hf, Zr, U and Th: implications for high field strength element depletions in island-arc basalts. *Earth Planet. Sci. Let.*, **128**:327-339.

Campos Neto M.C. 2000. Orogenic systems from Southwestern Gondwana: an approach to Brasiliano-Pan-African cycle and orogenic collage in Southeastern Brasil. **In:** U.G. Cordani, E.J. Milani, D.A. Campos (Eds.) *Tectonic evolution of South America*. Rio de Janeiro, 31st International Geological Congress, 2000, pp.335-368.

Condie K.C. 2001. *Mantle Plumes and their record in Earth History*. Cambridge University Press, 306p.

Cordery M.C., Davies J.F., Campbell I.H. 1997. Genesis of flood basalts from eclogite-bearing mantle plumes. *Journ. Geophys. Res.*, **102**:20179-20198.

Corrêa da Costa P.C., Girardi V.A.V., Teixeira W. 2002. Petrologia dos diques máficos da região de Crixás–Goiás, porção centro-oeste do Estado de Goiás. **In:** SBG, Congresso Brasileiro de Geologia, 41, João Pessoa – PB, *Anais*, p.418.

Corrêa da Costa P.C., Girardi V.A.V., Teixeira W. 2003. Geoquímica isotópica (Sr e Nd) e geocronologia Rb/Sr - $^{40}Ar/^{39}Ar$ dos diques máficos de Goiás. **In:** SBGq, Congresso Brasileiro de Gequímica, 9, Belém – PA, *Resumos Expandidos*, p.417.

Corrêa da Costa P.C. 2003. *Petrologia, geoquímica e geocronologia dos diques máficos da região de Crixás-Goiás, porção centro-oeste do Estado de Goiás*. Tese de Doutorado - Instituto de Geociências, Universidade de São Paulo, São Paulo-SP, 151p.

Corrêa da Costa P.C. & Girardi V.A.V. 2004. Petrografia e química mineral dos diques máficos da região Crixás-Goiás, Estado de Goiás. *Geologia USP – Série Científica*, **4**(2):27-42

Correia C.T. & Girardi V.A.V. 1989. Estudo geoquímico e petrológico dos anfibolitos da região de Cássia, MG. *Rev. Bras. Geoc.*, **19**:37-50.

Correia C.T. 2001. *O Método Re-Os e o estudo da origem e evolução tectônica dos grandes complexos máficos-ultramáficos, do centro-oeste do Brasil*. Tese de Livre-Docência, Instituto de Geociências, Universidade de São Paulo, São Paulo-SP, 59p.

DePaolo D.J. 1981. Trace element and isotopic effects of combined wall rock assimilation and fractional crystallisation. *Earth Planet. Sci. Let.*, **53**:189-202.

Dickin A.P. 1997. Radiogenic Isotope Geology. Cambridge Universit Press. New York, p. 133-201.

Ellam R. M. & Cox K. G. 1989. A Proterozoic lithospheric source for Karroo magmatism: evidence from the Nuanetsi picrites. *Earth Planet. Sci. Let.*, **92**:207-218.

Faure G. & Hurley P.M. 1963. The isotopic composition of strontium in oceanic and continental basalt: application to the origin of igneous rocks. *Journ. Petrology*, **4**:31-50.

Franzini M., Leoni L., Saitta 1975. Revisionne di una metodologia analitica per fluorescenza-X, basata sulla correzione completa degli effeti di matrice. *Rend. Soc. It. Mineral. Petrol.*, **31**:365-378.

Girardi V.A.V., Mazzucchelli M., Molesini M., Finatti M.C., Rivalenti G., Correia C.T. 1992. Petrological and geochemical aspects of mafic dykes of Goiás State, Brazil. **In:** SBG, Congresso Brasileiro de Geologia, 37, São Paulo-SP, *Anais*, **1**:490-495.

Girardi V.A.V., Mazzucchelli M., Molesini M., Civetta L., Petrini R., Bossi J., Campal N., Teixeira W., Correia C. T. 1996. Petrology and geochemistry of the mafic dyke swarm of the Treinta Y Treis region, Northeast Uruguay. *Journ. South Amer. Earth Sci.*, **9**:243-249.

Hart S. 1988. Heterogeneous mantle domains: signatures, genesis and mixing chronologies. *Earth Planet. Sci. Let.*, **90**:273-296.

Hasui Y. & Almeida F.F.M. de A. 1970. Geocronologia do Centro-Oeste Brasileiro. *Bol. da Sociedade Brasileira de Geologia*, **19**(1):5-26.

Helffrinch G.R. & Wood B.J. 2001. The Earth's mantle. *Nature*, **412**:501-507.

Hergt J. M., Peate D. W., Hawkesworth C. J. 1991. The petrogenesis of the Mesozoic Gondwana low-Ti flood basalts. *Earth Planet. Sci. Let.*, **105**:134-148.

Iacumin M., Piccirillo E.M., Girardi V.A.V., Teixeira W., Bellieni G., Echeveste H., Fernandez R., Pinese J.P.P., Ribot A. 2001. Early Proterozoic calc-alkaline and Middle Proterozoic tholeiitic dike swarms from Central-Eastern Argentina: petrology, geochemistry,

Sr-Nd isotopes and tectonic implications. *Journ. Petrology*, **42**:2109-2143.

Iacumin M., De Min A., Piccirillo E.M., Bellieni G. 2003. Source mantle heterogeneity and its role in the genesis of Late Archaean–Proterozoic (2.7–1.0 Ga) and Mesozoic (200 and 130 Ma) tholeiitic magmatism in the South American Platform. *Earth Planet. Sci. Let. - Reviews*, **62**:365–397.

Jaques A.L. & Green D.H. 1979. Determination of liquid compositions in high-pressure melting of peridotite. *American Mineralogist*, **64**:1312-1321.

Kawashita K. 1972. *O método Rb/Sr em rochas sedimentares: aplicação para as bacias do Paraná e Amazonas*. Tese de Doutorado, Instituto de Geociências, Universidade de São Paulo, São Paulo-SP, 111 p.

King S.D. & Anderson D.L. 1998. Edge-driven convection. *Earth Planet. Sci. Let.*, **160**: 289-296.

Kushiro I. 2001. Partial Melting Experiments on Peridotite and Origin of Mid-Ocean Ridge Basalt. *Ann. Earth Planet. Sci. Let. - Reviews*, **29**:71-107.

Kuyumjian R.M. 1991. Mafic dyke swarms in Goiás, central, Brazil. **In:** International Symposium on Mafic Dykes, São Paulo. *Extended Abstracts*. p. 51-54.

Kuyumjian R.M. 1998. Mafic Dyke Swarms of the Goiás Massif, Central Brazil. *Rev. Bras. de Geoc.*, **28**:45-50.

Lacerda Filho J.V. de, Rezende A., Silva A. da 2000. *Programa Levantamentos Geológicos Básicos do Brasil. Geologia e Recursos Minerais do Estado de Goiás e do Distrito Federal*. Goiânia, CPRM/METAGO/UnB, 184p.

Leitch A.M. & Davis G.F. 2001. Mantle plumes and flood basalts: enhanced melting from plume ascent and an eclogite component. *Journ. of Geophys. Res.*, **106**:2047-2059.

Leoni L. & Saitta M. 1976. X-ray fluorescence analysis of 29 trace elements in rocks and mineral standards. *Rend. Soc. It. Mineral. Petrol.*, **32**:497-510.

Ludwig K. R. 1999. *Isoplot/Ex version 2.10 (A Geochronological Toolkit for Microsoft Excel)*. Barkeley Geochronology Center, Spec. Public. 1a.

Mazzucchelli M., Rivalenti G., Piccirillo E., Girardi V.A.V., Civetta L. 1995. Petrology of the Proterozoic mafic dyke swarms of Uruguay and constraints on their mantle source composition. *Prec. Res.*, **74**:177-194.

Mazzucchelli M., Rivalenti G., Menezes Leal A.B., Girardi V.A.V., Brito Neves B.B., Teixeira W. 2001. Petrology of metabasaltic dykes in the Diamantina region, Minas Gerais, Brazil. *Per. di Mineralogia*, **70**:231-254.

McDonough W.F. & Sun S.S. 1995. The composition of the Earth. *Chemical Geology*, **120**:223-253.

Menezes Leal A.B., Bellieni G., Girardi V.A.V., Bastos Leal L.R., Teixeira W., Piccirillo E.M. 1995. Contribuição ao estudo petrológico e geoquímico dos enxames de diques máficos de Uauá, Bahia. *Geochim. Bras.*, **9**:61-90.

Menezes Leal A.B., Girardi V.A.V., Bastos Leal L.R. 2000. Petrologia e geoquímica do magmatismo básico da Suíte Básica Apoteri, Estado de Roraima - Brasil. *Geochim. Bras.*, **14**:155-174.

Pearce T.H. 1968. A contribution to the theory of variations diagrams. *Contr. Mineral. Petrol.*, **19**:42-57.

Philippot P. & Selverstone J. 1991 Trace-elements brines in eclogitic veins: implications for fluid composition and transport during subduction. *Contr. Mineral. Petrol.*, **106**:417-430.

Pimentel M.M., Jost H., Fuck R. A., Del'Rey Silva J.H. 1996. Dados Rb-Sr e Sm-Nd da região de Jussara-Goiás-Mosssamedes (GO), e o limite entre os terrenos antigos do Maciço de Goiás e o Arco magmático de Goiás. *Rev. Bras. Geoc.*, **26**:61-70..

Pimentel M.M., Jost H., Fuck R.A., Armstrong R.A., Dantas E.L., Portrel A. 2003. Neoproterozoic Anatexis of 2.9 Ga Old Granitoids in the Goiás-Crixás Archean Block, Central Brazil: Evidence from New U-Pb Shrimp data and Sm-Nd Isotopes. *Geologia USP – Série Científica*, **3**:1-12.

Pimentel M.M., Jost H., Fuck R. A. 2004. O embasamento da Faixa Brasília e o arco magmático de Goiás. **In:** Mantesso Neto V., Bartorelli A., Carneiro C.D.R., Brito Neves B.B. (Eds.) *Geologia do Continente Sul-Americano: evolução da obra de Fernando Flávio Marques de Almeida*, pp.355-358.

Pinese J.P.P. 1997. *Geoquímica, geologia isotópica e aspectos petrológicos dos diques máficos pré-cambrianos da região de Lavras (MG), porção sul do Cráton São Francisco*. Tese de Doutorado, Instituto de Geociências, Universidade de São Paulo, São Paulo-SP, 178p.

Queiroz C.L. 2000. *Evolução tectono-estrutural dos terrenos granito-greenstone belt de Crixás, Brasil Central*. Tese de Doutorado, IG-UnB, 209p.

Rapp R.P., Watson E.B., Miller C.F. 1991. Partial melting of amphibolite/eclogite and the origin of Archean trondhjemites and tonalites. *Prec. Res.*, **51**:1-25.

Reiners P.W. 2002. Temporal-compositional trends in intraplate basalt eruptions: Implications for mantle heterogeneity and melting processes. *Geochemistry Geophysics Geosystems: An Electronic Journ. of The Earth Sci.*, **3**:1-30.

Rivalenti G., Mazzucchelli M., Molesini M., Petrini R., Girardi V.A.V., Bossi J., Campal N. 1995. Petrology of Late Proterozoic mafic dikes in the Nico Perez Region, Central Uruguay. *Mineral. Petrol.*, **55**:239-263.

Rivalenti G., Mazzucchelli M., Girardi V.A.V., Cavazzini G., Finatti C., Barbieri M.A., Teixeira W. 1998. Petrogenesis of the Paleoproterozoic basalt–andesite–rhyolitedyke association in the Carajas region, Amazonian craton. *Lithos*, **43**:235–265.

Sato K., Tassinari C.C.G., Kawashita K., Petronilho L. 1995. O método geocronológico Sm-Nd no IG/USP e suas aplicações. *Anais da Acad. Bras. Ciências*, **67**:313-336.

Saunders A.D., Storey M., Kent R.W., Norry M.J. 1992. Consequences of plume-lithosphere interactions. **In:** B.C. Storey, T. Alabaster, R.J. Pankhurst (Eds.) *Magmatism and the Causes of Continental Break-up*, p.41-60.

Sheraton J. W. & Black L. P. 1981. Geochemistry and geochronology of Proterozoic tholeite dykes of East Antarctica: evidence for mantle metasomatism. *Contr. Mineral. Petrol.*, **78**:305-317

Stormer J.C. & Nicholls J. 1978. XLFRAC: a program for interactive testing of magmatic differentiation models. *Computers and Geoscience*, **4**:143-159.

Sun S.S. & McDonough W.F. 1989. Chemical and isotopic systematics of oceanic basalts: implications for mantle composition and process. **In:** Saunders, A.D., Norry, M.J. (Eds.) Magmatism in the Ocean Basins. *Geol. Soc. Spec. Publ.*, **42**:313-345.

Takahashi E. & Kushiro I. 1983. Melting of dry peridotite at high pressures and basalt magma genesis. *Am. Mineral.*, **68**:859-879.

Takahashi E., Nakajima K., Wright T. L. 1998. Origin of the Columbia

River basalts: melting model of a heterogeneous plume head. *Earth Planet. Sci. Let.*, **162**:63-80.

Tassinari C.C.G. & Montalvão R.M.G. 1980. Estudo Geocronológico do *greenstone belt* de Crixás. **In:** SBG, Congresso Brasileiro de Geologia, 31, Camboriú-SC, *Anais*, p.2759.

Tatsumoto M. & Nakamura Y. 1991. Dupal anomaly in the sea of Japan: Pd, Nd, and Sr isotopic variations at the eastern Eurasian continental margin. *Geoch. Cosmoch. Acta*, **55**:3697-3708.

Teixeira L.R. 1997. Genesis versão 2.0. Aplicativo de modelamento geoquímico. Bahia, Brasil.

Teixeira W. 1990. The Proterozoic mafic dyke swarms and alkaline intrusions in the Amazonian Craton, South America, and their tectonic evolution based on Rb-Sr, K-Ar and Ar-Ar geochronology. **In:** A.J. Parker, P.C. Rickwood, D.H. Tucker (Eds.) *Mafic Dykes and Emplacement Mechanisms. Balkema*, **23**:285-293.

Teixeira W., Renne P.R., Bossi J., Campal N., D'Agrella Filho M.S. 1999. ^{40}Ar–^{39}Ar and Rb–Sr geochronology of the Uruguayan dike swarm, Rio de la Plata Craton and implications for Proterozoic intraplate activity in western Gondwana. *Prec. Res.*, **93**:153–180.

Tomazzoli E.R. 1992. O *greenstone belt* de Goiás: estudos geocronológicos. *Rev. Bras. Geoc.*, **22**:56-60.

Tomazzoli E.R. 1997. *Aspectos geológicos e petrológicos do enxame de diques Morro Agudo de Goiás*. Tese de Doutorado, IG-UnB, Brasília, 293p.

Vargas M.C. 1992. *Geologia das rochas granito-gnáissicas da região de Crixás, Guarinos, Pilar de Goiás e Hidrolina, Goiás*. Dissertação de Mestrado, IG-UnB, 172p.

Weaver B. L. 1991. The origin of ocean island basalt end-member compositions: trace element and isotopic constraints. *Earth Planet. Sci. Let.*, **104**:381-397.

Weaver B. L., Wood D. A., Tarney J., Joron J. L. 1987. Geochemistry of ocean islands basalts from South Atlantic: Ascension, Bouvet, St. Helena., Gough and Tristan da Cunha. **In:** Fitton J. G., Upton B. G. (Eds.) Alkaline igneous rocks. *Geol. Soc. Spec. Publ.*, **30**:253-267.

Zhao J-x & Mc Culloch M. T. 1993. Melting of a subduction-modified continental lithospheric mantle: evidence from Late Proterozoic mafic dike swarm in central Australia. *Geology*, **21**:463-466.

Zindler A. & Hart S. 1986. Chemical geodynamics. *Ann. Earth Planet. Sci. Let. - Reviews*, **14**:493-571.

Manuscrito A-1526
Recebido em 19 de agosto de 2004
Revisão dos autores em 15 de dezembro de 2004
Revisão aceita em 20 de dezembro de 2004